A newly designed demagnetization furnace for paleomagnetic thermal treatment with highly attenuated inside magnetic field intensity

Huafeng Qin[1], Xiang Zhao[1, 2], Shuangchi Liu[1], Greig A. Paterson[3,4], Zhaoxia Jiang[1,5], Shuhui Cai[1], Jinhua Li[3], Qingsong Liu[1,6], Rixiang Zhu[1]

[1] *State Key Laboratory of Lithospheric Evolution, Institute of Geology and Geophysics, Chinese Academy of Sciences, Beijing 100029, China*

[2] *Research School of Earth Sciences, Australian National University, Canberra, ACT 2601, Australia*

[3]*Key Laboratory of Earth and Planetary Physics, Institute of Geology and Geophysics, Chinese Academy of Sciences, Beijing 100029, China*

[4] *Department of Earth, Ocean and Ecological Sciences, University of Liverpool, Liverpool L69 7ZE, UK*

[5] *Key Laboratory of Submarine Geosciences and Prospecting Techniques, Ministry of Education, and College of Marine Geosciences, Ocean University of China, 266100 Qingdao, P.R. China*

[6] *Department of Marine Science and Engineering, Southern University of Science and Technology, Shenzhen 518055, China*

Abstract

Thermal demagnetization furnaces are routine facilities that underpin countless paleomagnetic studies by allowing the progressive removal of naturally acquired magnetic remanence or the imparting of well controlled laboratory magnetization. The ideal thermal demagnetizer should maintain “zero” magnetic field during thermal treatments. However, magnetic field noise, including residual magnetic fields of material used to construct the furnace and induced fields caused by the heating current in the furnace are always present. As technology advances allowing the measurement of ever weaker magnetic remanences, it is essential that high-performance demagnetization furnaces are developed to reduce these sources of magnetic

field noise. By combining efficient demagnetization of shielding and a new structure of heating wire, we have developed a new demagnetization furnace with low magnetic field noise. Repeated progressive thermal demagnetization experiments using specimens that were previously completely thermally demagnetized above their Curie temperature were carried out to explore the effects of fields within various types of furnace during demagnetization. These experiments confirm that magnetic field noise in various furnaces can have an observable and detrimental impact on demagnetization behavior and that this is reduced with our new design. The new heating element design and procedure for reducing magnetic field noises represent a significant improvement in the design of thermal demagnetizers and allows for extremely weak specimens to be successfully measured.

Plain language summary

Earth magnetic field had played a significant role to the lives on Earth. Studying how and when Earth magnetic field generated and how it evoluted in the ancient time will provide key information of plantery evolution and life evolution. Thermal demagnetization of nature remanent magnetization carried by geological material is one of the ways to obtain the ancient magnetic field information. The thermal demagnetization furnace plays important role in such studies. An ideal thermal furnace for this purpose should maintain a “zero” magnetic field inside the sample chamber during the whole process. Reducing the residual magnetic field of the furnace itself and the induced field caused by the heating element is the key to making a high-performance demagnetization. We have developed a new demagnetization furnace could significant reduce the magnetic field noises, which represent an important improvement in the design of thermal demagnetizers and allows for extremely weak specimens to be successfully thermal demagnetized.

Key words:

Paleomagnetism, thermal demagnetization, furnace, AC magnetic field, residual magnetic field，heating wire structure

1. Introduction

Paleomagnetism investigates the geomagnetic field through geologic time by the measurement of remanent magnetizations recorded by magnetic minerals in natural materials. The natural remanent magnetization (NRM) usually consists of multiple components. Therefore, to define the stable characteristic remanent magnetization (ChRM) of geological interest, any secondary remanent magnetization needs be removed using partial demagnetization techniques (e.g., the step-wise progressive thermal or alternating field demagnetization [Irving et al., 1961; Schmidt, 1993]). During thermal demagnetization, specimens are heated to a pre-selected temperature, held for a period of time (e.g., 10-30 minutes), and then cooled down to the room temperature in "zero" magnetic field environment [Collinson, 1983]. This treatment will be conducted repeatedly with progressive increased target temperature till the ChRM is isolated [Thellier, 1966; Collinson, 1975]. Thermal demagnetization is one of the standard demagnetization methods, and thermal demagnetization furnaces (or thermal demagnetizers) are present in nearly all paleomagnetic laboratories.

Although widely used, the experimental success rate of thermal demagnetization can be relatively low for weak sedimentary rocks. It is often found that remanent direction of some specimens become distorted at high temperatures, but the ChRM can still be obtained by alternating demagnetization using sister specimens. The failure of thermal demagnetization could be attributed to irreversible thermal physio-chemical alterations upon heating [e.g., Wasilewski 1969, Heller et al., 1970], partial thermoremanent magnetization (pTRM) acquisition in the presence of a residual DC field upon cooling [Collinson, 1975], or magnetic fields caused by the heating current (Heller et al., 1970). Alternatively, a weak field high temperature isothermal remanence could be acquired when the current field is shut off abruptly at the end of heating [Zheng et al., 2010]. Similarly, it is also possible to acquire a high temperature anhysteretic remanent magnetization in the presence of DC residual field imposed on the alternating field (AF) generated by the AC supply used to power the heating elements [Zheng et al., 2010]. Thus, a combination of these effects could seriously distort the paleomagnetic results. Although early studies could not detect differences between inductive and noninductive heating wire [Irving et al., 1961], inductive AF can cause unwanted AF demagnetization at high temperature. Given that the coercivity of magnetic minerals reduces quickly as the temperature approaches the unblocking

temperature or Curie temperature, this effect may be substantial. In the extreme, the NRM direction may be changed abnormally by single axis AF demagnetization because of the stationary current field [Stephenson, 1983] or through the acquisition of gyroremanence [Stephenson, 1983, Finn and Coe, 2016] at high temperature.

Reducing the fields present in thermal demagnetizers can significantly improve the quality of paleomagnetic measurements, particularly for weakly magnetized specimens. Moreover, for the study of meteorites in planetary science or magnetizations acquired near the onset of the geodynamo, understanding the characteristic remanent magnetization acquired in low magnetic fields, including extremely weak fields (nT range) is a topic of great interest [Weiss et al., 2010; Tarduno et al., 2015]. It is important that the technology around thermal demagnetizers progresses to keep pace with the change demands of the scientists who use them.

In this study, we will first describe the technology to reduce the residual magnetic field for a newly designed thermal demagnetizer, including improvement of degaussing approach for the shield cylinder and a new structure of heating element as well as an improved temperature control. We then conduct detail experiments to test the performance of the new furnace in comparison to currently available commercial equivalents.

2. New design of furnace for thermal demagnetization

2.1 Degaussing the shield cylinder

In order to shield the influence of external magnetic field, the chamber of thermal demagnetization furnace is usually installed in a magnetic shield cylinder. The residual fields in sample zone vary from several nT to 150 nT in different furnaces [Paterson et al., 2012], which is mainly determined by the remanent magnetization of magnetic materials within the furnace [Freake and Thorp, 1971, Thiel et al., 2007]. Such remanences can be usually demagnetized by a stand-alone degaussing wand or by a solenoid coil wound around the outer surface of the shield cylinder. A degaussing wand consists of a copper coil produces an alternating magnetic field by applying a constant AC voltage. When the wand is slowly moved away, the effective alternating magnetic field decay and performs an alternating field demagnetization process on the degaussing

target. However, the unsteady movement of the wand controlled by hand can result in incomplete demagnetization which prevent to achieve ideal low remanences. On the other hand, a conventional degauss coil wrapped outside the shield cylinder performes demagnetization by flowing through a gradually decreasing sinusoidal current (Figure 1a). In this system, the directions of degaussing fields are always along the long axis. It is still difficult to achieve an ideal low fields in practice. This could due to the large size of the coil which cause difficult to reach enough high peak field or the non-uniform effective field distribution inside the coil.

Early experiments found that the best shield demagnetization results were obtained by passing the AC current through conductors within the shield cylinders or by passing the current longitudinally through the shielding material itself [Herrmannsfeldt and Salsburg, 1964].A circular magnetic field perpendicular to the central longitudinal axis will be produced in the cylindrical shield if a current conducting straight wire is passed though the longitudinal center axis of the shield cylinder, however, this require very large current to reach a certain demagnetization level. In practice, we use a total of eight 4 mm^2 copper lines wound from inside to outside of the shield cylinder to form a large coil (Figure 1b), and connet to a transformer with a twisted-pair cable. The transformer has separated primary and secondary windings which can be pulled apart. Separating the windings will generate a nonlinear attenuation of the alternating current in the coil which performes an alternating demagnetization on shield cylinder. The residual magnetic field in the sample region can be as low as 1 nT (Figure 1c), which makes it possible to further reduce spurious fields during thermal demagnetization.

Although not adopted here, employing a toroidal degaussing coil to embody the shield cylinder may also improve the uniformity of the degaussing field over the volume of the shield compared to conventional solenoid coil. Vioget et al. [2013] showed that successive degaussing in three spatial directions of a magnetic shield room could reduce the ambient field significantly. The same principle, applied to a thermal demagnetizer, would suggest that both toroidal and solenoidal windings can be combined for more effective degaussing of thermal demagnetizer shields, but this requires experimental verification.

2.2 The design of heating wires using in the new furnace.

Unlike minimizing residual DC bias fields, the effects of the AC magnetic fields generated by the wire current cannot be simply shielded. The heating elements in thermal demagnetizers is typically constructed by non-inductive winding in order to minimize the AC demagnetization effect of the heating current [Chamalaun, 1964]. There are generally two types of non-inductive heater winding, one is a bifilar solenoid wrapped on a cylindrical form to heat specimens within (Figure 2a). This style of winding is widely used in small furnaces such as Sogo Fine-TD furnace in Japan [Zheng et al., 2010]. It is also used by in some Kapabridges and variable field translation balances (VFTBs) to heat specimens. In this configuration, the opposing currents of adjacent wires reduce the AC magnetic field. A disadvantage of this system, however, is that the specimen region has to be small in order to maintain a accepteable resistance and workable power comsumption.

An alternative method is to use solenoids arranged in opposite direction (Figure 2b) or wound into a spiral ring as is used furnaces manufactured by Magnetic Measurements (UK) or ASC Scientific (USA). It is usually assumed that the magnetic field generated by a uniform solenoid is only in the interior and both ends of the solenoid [Shaw, 2010], but this idealized and neglects the fact that in a real solenoid the wire loops (and current loops) are not perfectly circular, which results in non-zero external fields. For effective cancellation of the fields generated in each solenoid, this design requires that opposing solenoids are perfectly antiparallel. Imperfect alignment results in the small, but potentially significant AC fields when large currents are applied during heating [Zheng et al., 2010a, b; Shaw, 2010].

From the Bio-Savart law in a cylindrical coordinate system (*see detail in supporting information*), it can be shown that the external magnetic field far from a solenoid is similar to that of one straight wire oriented along the length of the solenoid. So, if a straight wire is inserted into the center of a solenoid and is connected with the solenoid in series at one end, such that the current flow opposite to that in the solenoid, the opposing magnetic fields will partially cancel. This type of wire arrangement, which we call a straight core solenoid, is shown in Figure 2c and is the form of the heating element used in our new design of thermal demagnetizer. In supporting information, we outline comparative measurements of the external field of a standard solenoid and a straight core solenoid. The stray magnetic field from the straight core solenoid design is much smaller than that of a standard solenoid with identical winding (26-535 nT compared to 6000-7000

nT measured at a distance of 2 cm from the solenoid wire). We use this new heating element to build a new furnace named TD-PGL-100. When adjacent elements are arranged in opposite directions (Figure 2c) the magnetic field is about 130 nT in the heating chamber when applied 1A current in heating wire. For comparison, Zheng et al. (2010a, b) report similar 1A heating element fields for the commercially available Sogo Fine-TD, Magentic Measurements MMTD80 as ~240 and 840 nT, respectively. They also report 0.5 A heating element fields for the ASC TD48 and Natsuhara as being 3600 and 3200 nT, respectively.

2.3 Temperature control and and TD-PGL-100

Employing adjustable voltage silicon controlled rectifier (Fig 3a) over solid-state relay allows the output power to be decreased as the temperature approaches the target point which would help to avoid temperature overshootings. With carefull PID tunning, the oven has 1°C accuracy with a resolution of 0.1°C of temperature. As the examples of heating and cooling curves shown in the figure 3b, the temperature rises rapidly at the beginning of heating, and gradually approaches the target temperature after ~30 minutes and then the temperature is maintained for a certain time to ensure the samples are thoroughly heated. The cooling fan can be turned on manually or automaticly to cool the samples down. The temperature dropped rapidly and became slow when near room temperature. The heating and cooling data can be logged into USB memory automaticly, which is essential for the thermal treatment and related experiments espeically for absolute paleointensity studies.

A new furnace named TD-PGL-100 had been built based on all above mentioned techniques, which chamber has 120 cm length and 9 cm diameter, and the sample zone is desigened as 60 cm in length which allows up to 100 standard paleomagnetic specimens be treated in once. Temperature gradient in the sample zone is within 10°C of target temperature below 600°C and 12°C at 700°C

3. Thermal demagnetization experiments

3.1 Specimen description and thermal demagnetizers

To verify the thermal demagnetization performance of our new furnace, we explored the

thermal demagnetization behavior of synthetic hematite specimens. Hematite specimens synthesized in the lab were chosen to avoid potential thermochemical changes during multiple heatings. The particles of hematite are cubic and with a broadly uniform size distribution with an average length and width of 570 nm and 545 nm, respectively (*see Supplementary Information*). In addition, the weak magnetizations of hematite are suitable for checking the effects of weak background fields.

Eight synthetic specimens were prepared by mixing hematite with quartz sand (5 g), Kaolinite (5 g) into 20 ml deionized water in water. The mixtures were then loaded into ceramic boxes (2×2×2 cm) and allowed to dry and consolidate in ambient atmosphere Five of the specimens contained more hematite were classified as strong specimens (D2-1, 2, 4-6), and the other three contained less hematite are classified as weak specimens (D2-7,8,12).

To investigate if these demagnetization experiments are influenced by undesirable magnetic fields from the furnace, we adopt a different style of thermal demagnetization procedure. Progressive thermal demagnetization of TRM was carried out to identify the unblocking temperature spectrum of the studied specimens. This was performed in an MMTD-SC paleointensity furnace.

Subsequently, specimens were heated to 700°C for complete thermal demagnetization, then the progressive thermal demagnetization was repeated. This was performed using two different demagnetization furnaces: an ASC Scientific TD48 and our new TD-PGL-100. If the specimens were fully demagnetized without the effects of stray magnetic fields in the furnace, the remanent magnetization of completely demagnetized specimens would remain unchanged during subsequent progressive demagnetization experiments. Finally, in order to quantitatively evaluate the influence of the background magnetic field, we assess the linearity of TRMs acquired in different applied magnetic field, especially in low DC bias fields using MMTD-SC.

We also carried out comparative thermal demagnetization experiments on some natural specimens. Two groups of sister specimens were heated using the two different demagnetization furnaces. Remanent directions and moments were measured with a cryogenic magnetometer system (2G Enterprises 755) installed in the magnetically shielded room with residual field < 300

nT at IGGCAS. Background noise is typically lower than $2\times10^{-12}Am^2$, and the background moment of the sample tray was kept less than $5\times10^{-11}Am^2$ during the measurements. All the experiments were completed in the paleomagnetic laboratory at the Institute of Geology and Geophysics, Chinese Academy of Sciences (IGGCAS).

3.2 Thermal demagnetization of TRM

A full TRM was acquired by cooling specimens from 700°C in the presence of a 30 μT field using the MMTD-SC paleointensity furnace, then progressive thermal demagnetization was performed by removing the applied field. The amplitudes of the TRMs range from 1.13×10^{-6} Am^2 to 0.65×10^{-6} Am^2 for strongly magnetic specimens and from 1.52×10^{-7} Am^2 to 1.88×10^{-7} Am^2 for weakly magnetic specimens. Subsequently, specimens were subject to stepwise progressive thermal demagnetization up to 700°C in our new furnace.

During demagnetization we used temperature intervals of 100°C below 500°C and 10°C above 600°C. After each heating and cooling step, remanences were measured. The results are shown in Figure 4. The intensities of remanent magnetization of all specimens did not change significantly until 600°C, and began to reduce rapidly above 640 (Figure 4a-e), which indicate the distribution of unblocking temperatures is relatively narrow which is consistent with narrow size distribution of hematie. For the weak specimens, there are small inflection around 580-600°C which indicate that these samples could have a small amount of magnetite. The inflection actually present in strong specimens as well, but the signal is buried by the relatively strong total magnetization. We note that two specimens (D2-1, D2-2), which were placed on the door side of the furnace, are complete demagnetization at 680°C, but other specimens are demagnetized by the 670°C step. This is possibly caused by thermal gradients in the sample zone.

Orthogonal projection diagrams [Zijderveld 1967] indicate that the directions shift a little at low temperatures, but this is likely due to measurement errors and manual handling of the specimens between steps. The magnetic moments of terminal demagnetization steps are less than one percent of initial total TRM and lie close to the origin of the plots (the inserts in Figure 4).

3.3 Comparisons of repeated progressive thermal demagnetization behavior for different

furnaces

The repeated thermal demagnetization experiment is carried out after the specimens were heated up to 700°C for complete demagnetization. We first carried out this experiment using ASC TD48 dual chamber thermal demagnetizer. We aimed to keep specimens in the same angle and position while placing them on the sample holder during heating and cooling in the furnace. Since the magnetic moments are relatively weak, the sample holder of the cryogenic magnetometer was cleaned before each measurement, and the measurement is repeated twice and the drift value was kept less than $5.0\times10^{-11}Am^2$. The experimental results are shown in Figure 5. The magnetic moments of the initial demagnetized state range from $4.38\times10^{-10}Am^2$ to $1.32\times10^{-9}Am^2$ for strong specimens and from $7.7\times10^{-11}Am^2$ to $1.69\times10^{-10}Am^2$ for weak specimens. These values are just 0.05–0.12% of initial TRM acquired in 30 μT. In the subsequent progressive demagnetization experiments, the intensities and directions of remanence remain stable below 640°C, despite noisy due to the weak moments. Above ~650°C, however, the moments rapidly increase and reach peak values at 670–680°C. The maximum magnetic moments are an order of magnitude greater than that the initial demagnetization state. The magnetic moments decrease again after further heating to 690°C and 700°C.

For specimens, directions of the spurious moments are identical, which suggests that they are susceptible to the to a global cause. It is no doubt that the extra undesirable remanence acquired during the thermal demagnetization process, and those spurious moments are not only affected by the weak residual field, but very likely related to the noise magnetic field of AC current. However, even the worst the superimposed remanence acquired in re-demagnetization experiments is still very small compared to total TRM acquired in 30 μT, The maximum value obtained is just about 2% of a TRM in 30 μT.

We repeated the same modified progressive thermal demagnetization experiments using the TD-PGL-100 furnace. The experimental results are shown in Figure 6. First of all, the remanence moments after the first heating up to 700°C are lower than the value of completely demagnetization using TD48 furnace, which is due to the lower residual fields in the TD-PGL-100 furnace. The initial moments range from $6.5\times10^{-11}Am^2$ to $2.8\times10^{-10}Am^2$ for strong specimens and

from $2.5\times10^{-11}Am^2$ to $9.4\times10^{-11}Am^2$ for weak specimens. These are about 0.02-0.05% of the 30 μT TRM. These experiments also confirm that the specimens have relatively stable (within the limits of noise) moments below 640°C (Figure 6). For our new furnace, the magnetic moments and directions of all specimens also clearly change in the 650-700ºC temperature interval, indicating that our new thermal demagnetizer is also affected by field noise. We note, however, that the changes in the magnetic moments are much less than those seen using the ASC TD-48 furnace and typically an order of magnitude smaller. Some of the magnetic moments do not always increase, but also decrease (e.g., Figure 6a, b). It is possible due to the superimposed remanence caused by the noise field is limited, and opposite with the previous remanence direction.

3.4 TRM acquisition in different fields

Spurious remanences caused by noise field can affect the effectiveness of thermal demagnetization, but will also have an impact on laboratory remanences acquired low fields. In order to quantitatively evaluate this effect, we also carried out total TRM acquisition experiments in 7 different fields ranging from 0.1 μT to 100 μT. The TRMs were produced by cooling form 700°C using the MMTD-SC paleointensity furnace. The TRM directions from the different applied field strengths are consistent, but the relationship between field strength and moment intensity is not a simple linear trend at low fields, as should be expected. The results are shown in the Figure 7. A linear field dependence of TRM was observed for specimens in the fields larger than 1 μT. At low fields (< 1 μT), however, it is more complex, which is similar to previous studies [e.g., Kletetschka et al., 2006]. This deviation from a linear trend may be related to limitations in controlling the precision of the magnetic field or may be related to mechanisms of TRM acquired in very weak fields [Dunlop and Argyle, 1997]. The trends, however, may also be due to the influence spurious magnetic fields in the furnace affecting TRM acquisition.

We also plot the magnetic moment variations of re-demagnetization experiments with different furnace in the Figure 7. The maximum superimposed noise magnetic moments in ASC TD48 is close to the TRM acquisition in ~1 μT. The magnetic moments after completely demagnetization have very low values, but still deviate from the linear trend. On the other hand, if

we used the linear relationship in the high field to extrapolate the equivalent TRM in very low field, the magnetic moments of specimens after completely demagnetized using TD-PGL-100 are similar TRM obtained in 10 nT. Part of this deviation from a linear trend is that the background and noise of 2G-755 is larger than the expected value.

3.5 Thermal demagnetization of natural specimens

Thermal demagnetization experiments were carried out on 12 nature specimens in each group using ASC TD48 and TD-PGL-100, respectively. Nine sandstone specimens denoted as "B" were collected from Cenozoic strata in Yunnan, and three muddy limestone specimens denoted as "CM" were from Tibet. The main magnetic carrier mineral of sandstone specimen is hematite [Li et al., 2017]. They have only a single univectorial component decaying steadily toward high temperature. It can be used to verify whether the results of synthetic specimens behave the same in natural specimens. The muddy limestone specimens also contain hematite and have multi-component characteristics of different temperature ranges.

The experimental results are shown in Figure 8. The demagnetization characteristics of sandstone specimens obtained from different demagnetization furnaces are similar at low temperature, but the remanence directions of some specimens are quite different above 660°C. The remanence directions do not changed much after demagnetization at high temperature using the new furnace (Figure 8b, d, f, h, j). The demagnetization data of TD48 furnace became confusing at temperature over 660°C. For limestone specimens, there is no difference in demagnetization data from one specimen, although the directions have obvious multi-component characteristics. The other two are quite different (Figure 8k, l). It is beyond the aim of this paper to make clear the reasons for the differences, but complex magnetization history and/or complex blocking behavior may be one possibility. Taken together, all of the demagnetization data indicate that lower remanent magnetizations can be more successfully isolated during thermal demagnetization using the new demagnetizing furnace.

4. Discussion

Thermal demagnetization results will be affected by the performance of thermal demagnetizers. It has been reported that the thermal demagnetization of TRM that was acquired in 1 μT can be seriously affected by AC current fields which can reach up to 1000 μT [Zheng et al., 2010]. In such cases samples can acquire high temperature isothermal remanences when the heating current is abruptly switched off for cooling purpose. The typically AC current field produced by most of thermal demagnetizers are lower than 100 μT. From repeated thermal demagnetization experiments, the spurious remanence induced by these fields is relatively small when compared to a total TRM acquired in Earth like fields. Even in the worst case, the superimposed remanence acquired in re-demagnetization experiments is just about 2% of TRM acquired in 30 μT field. It may not be sufficient to affect paleomagnetic investigations of volcanic rocks. However, considering that detrital remanence (DRM) is typically an order of magnitude weaker than TRM for same content of magnetic mineral [Fuller et al., 2002], such spurious fields may have a large impact on thermal demagnetization data obtained from sedimentray rocks. Other weakly magnetized materials such as those right in geomagnetic reversals or excursions may also be influenced significantly. It is also strong enough to have a notable effect TRMs acquired in less than 1 μT for some Meteorite or Extraterrestrial samples [Weiss et al., 2010].

Moreover, residual fields are ubiquitous in thermal demagnetizers and, when on the order of less than a few thousands of Earth-like field, are usually considered sufficiently low for most thermal demagnetization experiments. However, in rocks containing two magnetic phases, such as magnetite and hematite, it is possible for a spurious moment in the direction of the stray field to be acquired by the magnetite portion during cooling, which can mask the direction of the hematite [e.g, Chamalaun and Proath, 1967]. Such behavior could be prevalent in sedimentary rocks, and prevent successful resolution of the paleomagnetic directions. Through a longitudinal coil system, we have shown that it is easy to reduce residual fields to several nT or even less. This system can be applied to almost all types of commercially available thermal demagnetizers with the mu-metal shielding cylinders.

Although our improved heating element can greatly reduce the AC current field, it cannot completely eliminate it. If lower AC magnetic fields are required, the only alternative would be to heat the specimes outside of the primary electrical heating element region. This could be achieved

by heating the sample region by hot gas flow heated outside the sample region. This style of furnace can reduce AC current field to practically zero [Heller et al., 1971]. However, considering which need extra gas bottle and normally limited heating capacity of gas flow furnace. Our new TD-PGL-100 thermal demagnetizer with lower AC current field and super low residual magnetic fields is a reasonable choice for most of the lab.

5. Conclusions

Here we introduce a new heating element that composed of a straight wire inserted into solenoid and connected in series at one end, a configuration we call a straight core solenoid. Such a configuration can significantly reduce the stray magnetic fields generated when a current is applied to the heating element. We also outline a demagnetization procedure that can reduce the residual magnetic field in shield cylinder can be reduced to less than 1 nT in sample zone after demagnetization using current conducting multiple straight wires though the shield cylinder. We combine these new improvements to develop a new thermal demagnetizer, which has significantly reduced the AC induced and residual magnetic fields. This will allow the successful recover of weak magnetizations blocked at high temperatures and has applications in recovering sedimentary magnetizations, records of geomagnetic polarity reversals, signals of the earliest geodynamo, as well as extraterrestrial magnetizations. This new thermal demagnetizer has been running normally for three years in the IGCCAS laboratory, and results demonstrate its excellent performance especially for these weakly magnetic natural specimens [Jiang et al., 2017, Yan et al., 2018].

6. Acknowledgements

We thank Jie Yuan and Dr Shihu Li for providing the natural samples for testing. This work was supported by NSFC grants 41674073 and the Project of National Deep Exploration Technology and Experimental Research(Grant number:SinoProbe-09-02(201011079)). Original data related to this paper have been uploaded to the private workspace in MagIC database and will be made public on acceptance of the manuscript. For the purpose of review, data are available from https://earthref.org/MagIC/16831/0439ba2d-e530-4c4a-a5ac-61b3b67036ed.

References

386 Butler, R. F. (1998), *Paleomagnetism: Magnetic Domains to Geologic Terranes*. Blackwell.
387 ISBN: 0-86542-070-X.

388 Coe, R. S. (1967), Paleointensity of the earth's magnetic field determined from Tertiary and
389 Quaternary rocks. *Journal of Geophysical Research*, 72: 3247-3262.

390 Collinson, D.W. (1983), *Methods in Rock Magnetism and Paleomagnetism: techniques and*
391 *Instrumaentation*. London, Chapman and Hall.

392 Constable, C., & Tauxe, L. (1996), Towards absolute calibration of sedimentary paleointensity
393 records. *Earth and Planetary Science Letters*, 143: 269-274.

394 Cottrell, R. D., & Tarduno, J. A. (1999), Geomagnetic paleointensity derived from single
395 plagioclase crystals. *Earth and Planetary Science Letters*, 169: 1-5.
396 https://doi.org/10.1016/S0012-821X(99)00068-0

397 Freake S. M. & Thorp, T. L. (1971), Shielding of Low Magnetic Fields with Multiple Cylindrical
398 Shells. *Review of Scientific Instruments*, 42, 1411. http://doi: 10.1063/1.1684894

399 Fuller, M., Kidane, T. & Ali, J. (2002), AF demagnetization characteristics of NRM, compared
400 with anhysteretic and saturation isothermal remanence: an aid in the interpretation of
401 NRM. *Physics and Chemistry of the Earth*, 27, 1169-1177.

402 Gubbins, D. (1999), The distinction between geomagnetic excursions and reversals. *Geophysical*
403 *Journal International*, 137, F1-F3.

404 Herrmannsfeldt, W. B., & Salsburg, B. L. (1964), Demagnetization of Magnetic Shield in the
405 Presence of the Earth's Field, *Review of Scientific Instruments*, 35, 906. http://doi:
406 10.1063/1.1746861

407 Irving, E., Robertsou, W. A., Stott, P. M., Tarling, D., & Ward, M. A. (1961), Treatment of
408 partially stable sedimentary rocks showing planar distribution of directions of
409 magnetization. *Journal of Geophysical Research*, 66, 1927-1933.

410 Jiang，Z. X., Liu Q. S., Dekkers, M. J., Zhao, X., Roberts, A. P., Yang, Z. Y., Jin, C. S., & Liu, J.

X. (2017), Remagnetization mechanisms in Triassic red beds from South China. *Earth and Planetary Science Letters*, 479:219-230. https://doi.org/10.1016/j.epsl.2017.09.019

Kletetschka, G., Fuller, M. D., Kohout, T., Wasilewski, P. J., Herrero-Bervera, E., Ness, N. F., & Acuna, M. H. (2006), TRM in low magnetic fields: a minimum field that can be recorded by large multidomain grains. *Physics of the Earth and Planetary Interiors*, 154, 290-298. https://doi.org/10.1016/j.pepi.2005.07.005

Li, S., Yang, Z., Deng, C. L., He, H. Y., Qin, H. F., & Sun, L. (2017), Clockwise rotations recorded in redbeds from the Jinggu Basin of northwestern Indochina. *Geological Society of America Bulletin*,129, 1100-1122. https://doi.org/10.1130/b31637.1

Paterson, G. A., Biggin, A. J., Yamamoto, Y., & Pan, Y. X. (2012), Towards the robust selection of Thellier-type paleointensity data: The influence of experimental noise, *Geochemistry, Geophysics, Geosystems*, 13, Q05Z43. http://doi: 10.1029/2012GC004046

Pick, T., & Tauxe, L. (1993), Geomagnetic paleointensities during the Cretaceous normal superchron measured using submarine basaltic glass. *Nature*, 366: 238-242.

Riisager, P., & Riisager J. (2001), Detecting multidomain magnetic grains in Thellier palaeointensity experiments. *Physics of the Earth and Planetary Interiors*, 125(1-4): 111-117. https://doi.org/10.1016/S0031-9201(01)00236-9

Schmidt, P. W. (1993), Paleomagnetic cleaning strategies. *Physics of the Earth and Planetary Interiors*, 76: 169–178.

Shaw, J. (2010), Comment on “A new high-precision furnace for paleomagnetic and paleointensity studies: Minimizing magnetic noise generated by heater currents inside traditional thermal demagnetizers” by Zhong Zheng, Xixi Zhao, and Chorng-Shern Horng, *Geochemistry, Geophysics, Geosystems*, 11, Q11Y11. http://doi:10.1029/2010GC003211

Stephenson, A. (1980), A gyroremanent magnetisation in anisotropic magnetic material, *Nature*, 284(5751), 49-51.

437 Stephenson, A. (1983), Changes in direction of the remanence of rocks produced by stationary
438 alternating field demagnetization, *Geophysical Jounarl Royal Astronomical Society*, 73,
439 213-239.

440 Tarduno, J., Cottrell, R., & Smirnov, A. (2002), The paleomagnetism of single silicate crystals:
441 Recording geomagnetic field strength during mixed polarity intervals, superchrons, and
442 inner core growth. *Reviews of Geophysics*, 44: RG1002.
443 http://doi:10.1029/2005RG000189

444 Tarduno, J. A., Cottrell, R. D., Watkeys, M. K., & Bauch, D. (2007), Geomagnetic field strength
445 3.2 billion years ago recorded by single silicate crystals. *Nature*, 466: 657-660.
446 http://doi:10.1038/nature05667

447 Tarduno, J. A., Cottrell, R. D., & Watkeys, M. K. (2010), Geodynamo, Solar Wind, and
448 Magnetopause 3.4 to 3.45 Billion Years Ago. *Science*, 327: 1238-1240. http://doi:
449 10.1126/science.1183445

450 Tauxe, L. (2010), *Essentials of Paleomagnetism*. Berkeley: University of California Press.

451 Thellier, E. (1996), Methods and apparatus for alternating current and thermal demagnetization in
452 *Methods and Techniques in Geophysics*, vol. 2, edited by S. K. Runcorn, pp. 205-249,
453 Interscience, London.

454 Thellier, E., & Thellier O. (1959), Sur I'intensité du champ magnétique terrestre dans le passé
455 historique et géologique. *Annales de Geophysique*, 15: 285-378.

456 Thiel, F., Schnabel, A., Knappe-Grüneberg, S., Stollfuß, D., & Burghoff, M. (2007),
457 Demagnetization of magnetically shielded rooms. *Review of Scientific Instruments*, 78,
458 035106. http://dx.doi.org/10.1063/1.2713433

459 Voigt, J., Knappe-Grüneberg, S., Schnabel, A., Körber, R., Burghoff, M. (2013), Measures to
460 reduce the residual field and field gradient inside a magnetically shielded room by a
461 factor of more than 10, *Metrology and Measurement Systems*, 20, 239-248.

462 Weiss, B. P., Gattacceca, J., Stanley, S., Rochettte, P., & Christensen U R. (2010), Paleomagnetic

record of meteorites and early plantesimal Differentiation. *Space Science Reviews*, 152: 341-390. https://doi.org/10.1007/s11214-009-9580-z

Yan, Y., Huang, B., Zhang, D., Charusiri, P., & Veeravinantanakul, A. (2018), Paleomagnetic study on the Permian rocks of the Indochina Block and its implications for paleogeographic configuration and northward drifting of Cathaysialand in the Paleo-Tethys. *Journal of Geophysical Research: Solid Earth*, 123. https://doi.org/10.1029/2018JB015511

Yu, Y., & Tauxe, L. (2004), On the use of magnetic transient hysteresis in paleomagnetism for granulometry. *Geochemistry*, *Geophysics*, *Geosystems*, 6, Q01H14. http://doi: 10.1029/2004GC000839

Yu, Y., Tauxe, L., & Gee, J. S. (2007), A linear field dependence of thermoremanence in low magnetic fields. *Physics of the Earth and Planetary Interiors*, 162: 244-248. https://doi.org/10.1016/j.pepi.2007.04.008

Zheng, Z., Zhao, X., & Horng, C.-S., (2010a). A new high precision furnace for paleomagnetic and paleointensity studies: Minimizing magnetic noise generated by heater currents inside traditional thermal demagnetizers. *Geochemistry*, *Geophysics*, *Geosystems*, 11, Q04Y08. http://doi:10.1029/2010GC003100

Zheng, Z., Zhao, X., & Horng, C.S. (2010b), Reply to comment by John Shaw on "A new high-precision furnace for paleomagnetic and paleointensity studies: Minimizing magnetic noise generated by heater currents inside traditional thermal demagnetizers", *Geochemistry*, *Geophysics*, *Geosystems*, 11, Q11Y12. http://doi:10.1029/2010GC003295

Zhu, R. X., Pan, Y. X., & Coe, R. S., (2000). Paleointensity studies of a lava succession from Jilin Province, Northeastern China: Evidence of the Blake event. *Journal of Geophysical Research: Solid Earth*, 105(B4): 8305-8318. https://doi.org/10.1029/1999JB900448

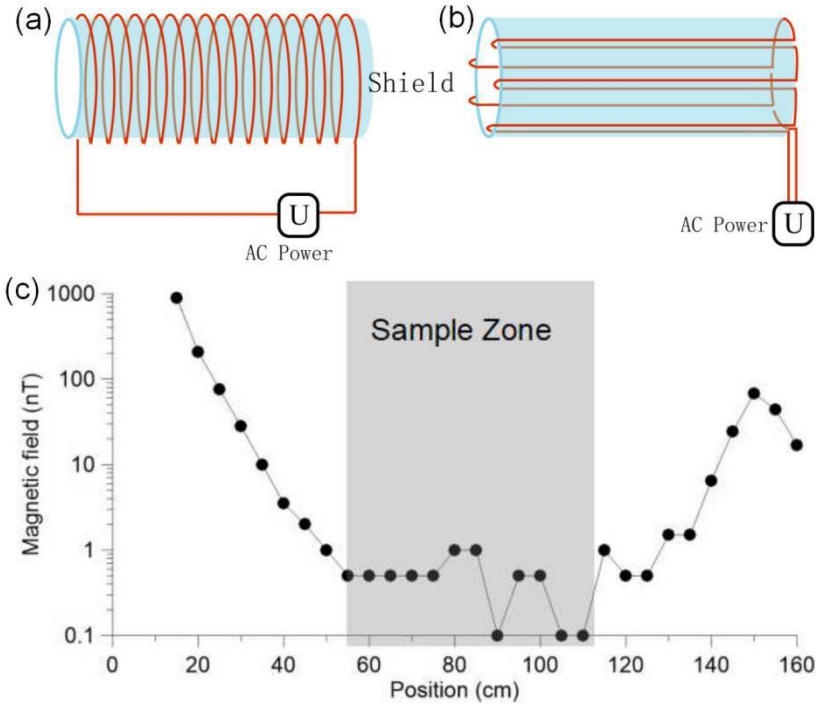

Figure 1. (a) A solenoidal and (b) toroidal degaussing coil embody the shield cylinder. (c) Residual fields along longitude axis in a shielding cylinder after demagnetization with winding method shown in part (b).

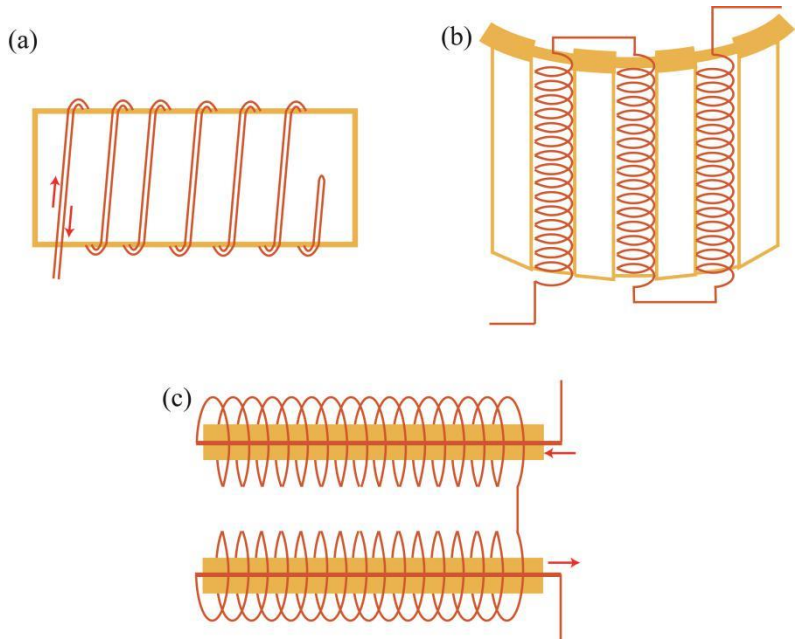

499

500

501 **Figure 2.** Configuration of non-inductive heating wires. (a) bifilar solenoid wrapped in small oven, (b)
502 solenoid-like spiral ring heating wires arranged in larger oven, (c) the new straight core solenoid
503 heating wires using in the TD-PGL-100

504

505

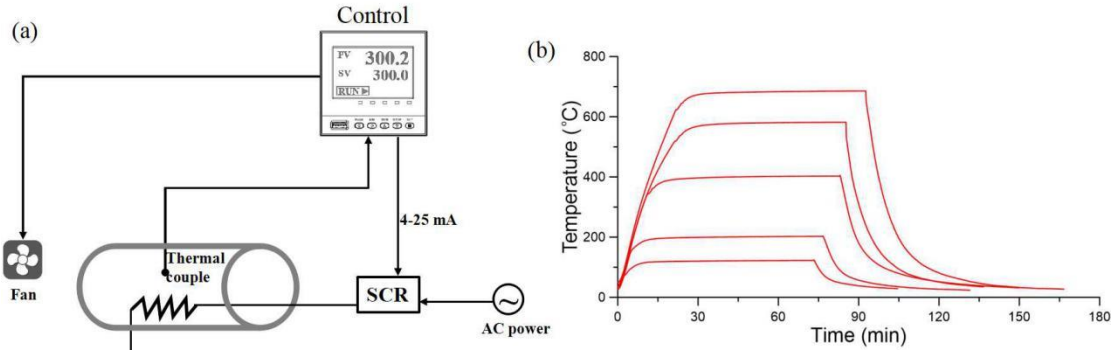

506

507 **Figure 3.** (a) Circuit schematic diagram for the TD-PGL-100. (b) Temperature curves during heating
508 and cooling at different target temperatures in a thermal demagnetization experiment.

509

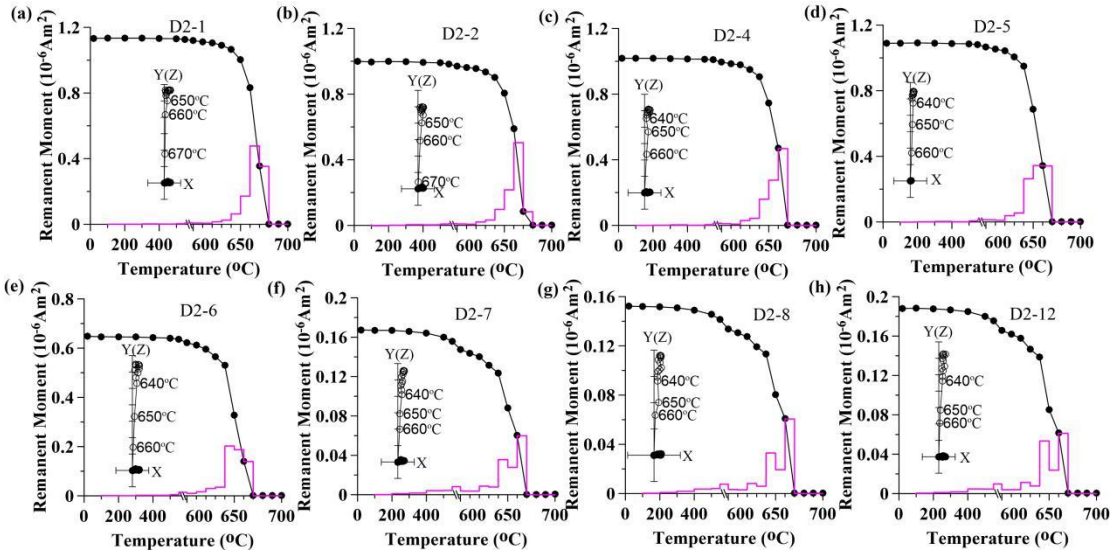

510

511 **Figure 4.** Thermal demagnetization curve (black symbol and line) and corresponding orthogonal plot
512 (inserts) of progressive thermal demagnetization of TRM (30 μT, 700°C) of synthetic specimens. Solid
513 (open) circles indicate projection on the horizontal (vertical) plane in orthogonal plot. The numbers
514 close to the symbols for the vertical planes projections indicate the level of stepwise demagnetization.
515 The purple line is the demagnetization proportion of individual temperature

516

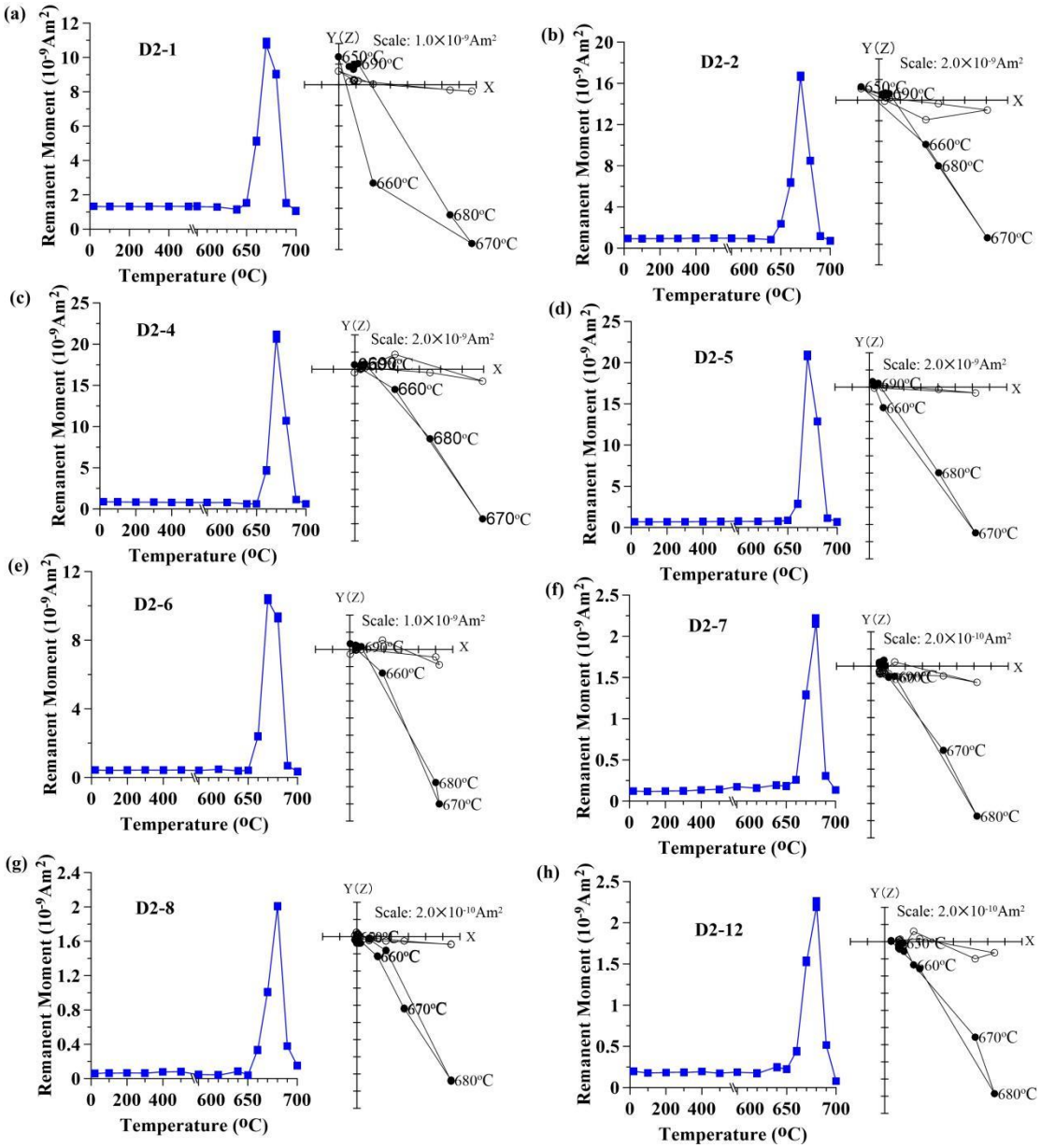

Figure 5. The thermal demagnetization curve (blue symbol and line, left) and corresponding orthogonal plot (right) of repeated progressive thermal demagnetization of the synthetic hematite specimens using the ASC TD48. Solid (open) circles indicate projection on the horizontal (vertical) plane.

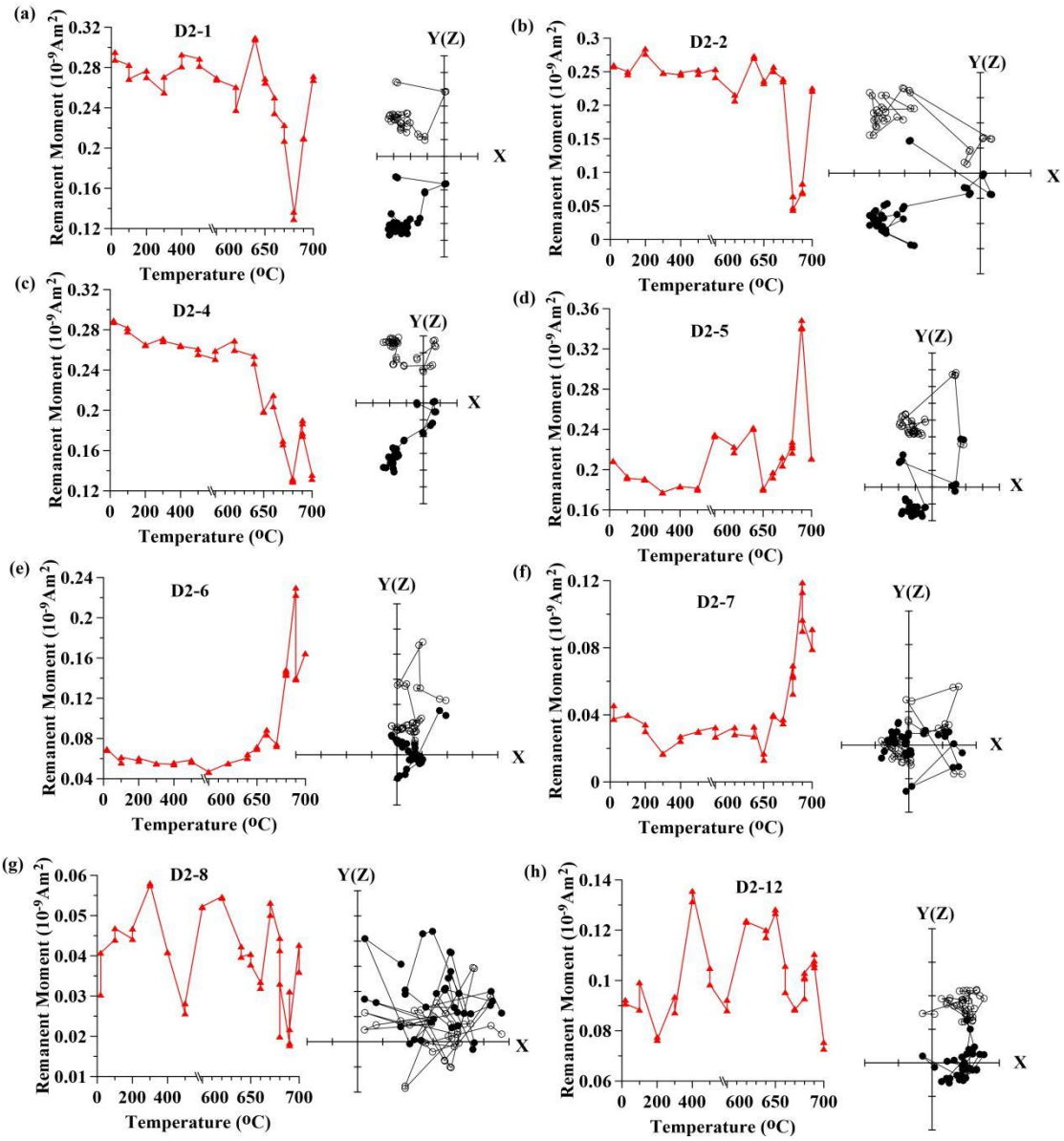

Figure 6. The thermal demagnetization curve (red symbol and line, left) and corresponding orthogonal plot (right) of repeated progressive thermal demagnetization of the synthetic hematite specimens using the TD-PGL-100. Solid (open) circles indicate projection on the horizontal (vertical) plane.

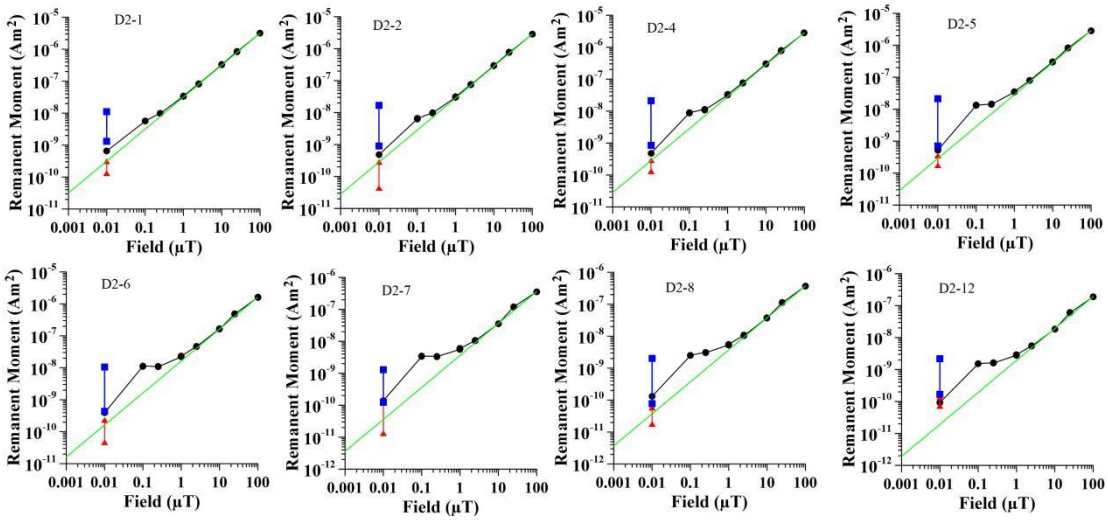

530

531 **Figure 7.** The magnetization of TRM dependence on applied magnetic field. Green lines indicate trend

532 fitting line. The blue squares (red triangles) indicate the variation range of thermal demagnetization in

533 Fig. 5 (Fig. 6)

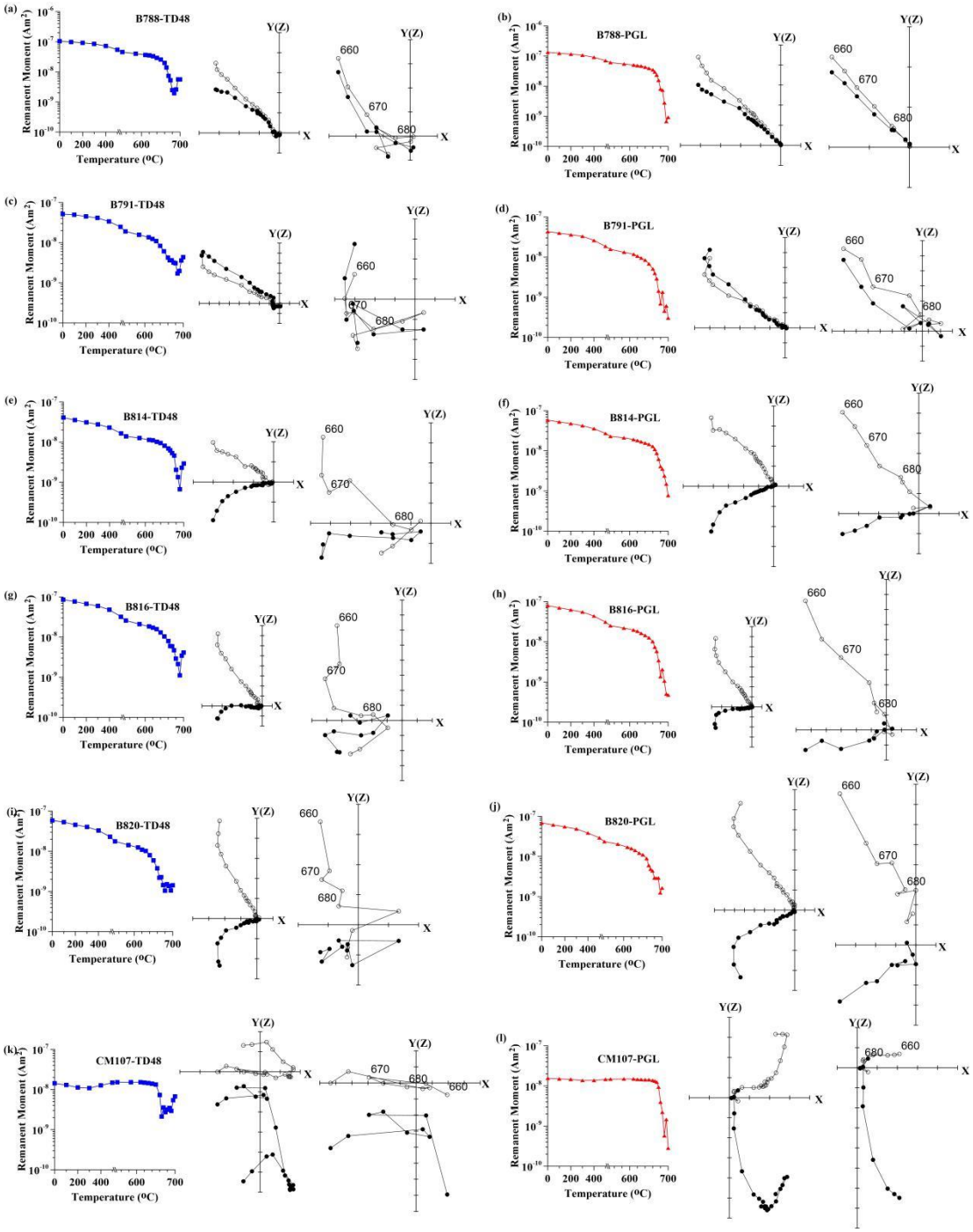

534

535 **Figure 8.** Thermal decay curve and corresponding orthogonal plot of progressive thermal
536 demagnetization of natural specimens. Blue squares represent the demagnetization data from the ASC
537 TD48, and the red triangles represent data from the TD-PGL-100. Solid (open) circles indicate
538 projection on the horizontal (vertical) plane.

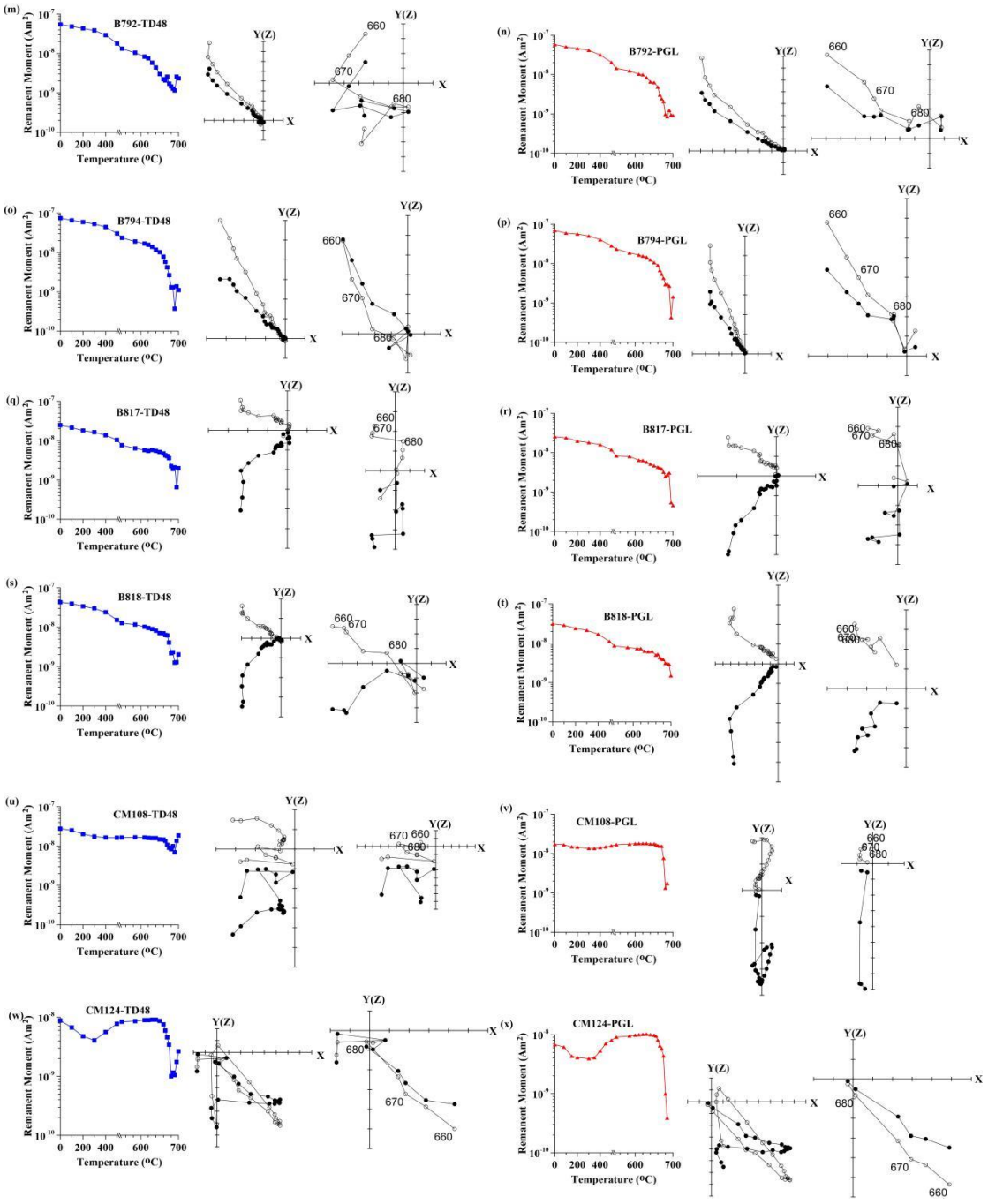

539

540 **Figure 8.** (continued)

Figure 1.

(a)

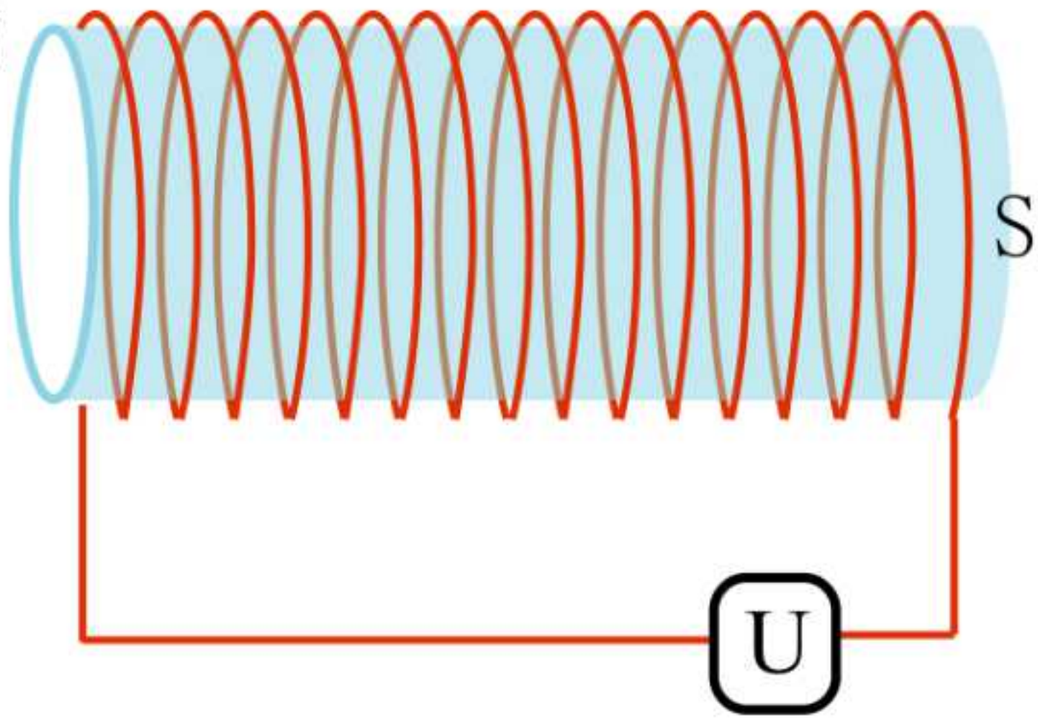
Shield
U
AC Power

(b)

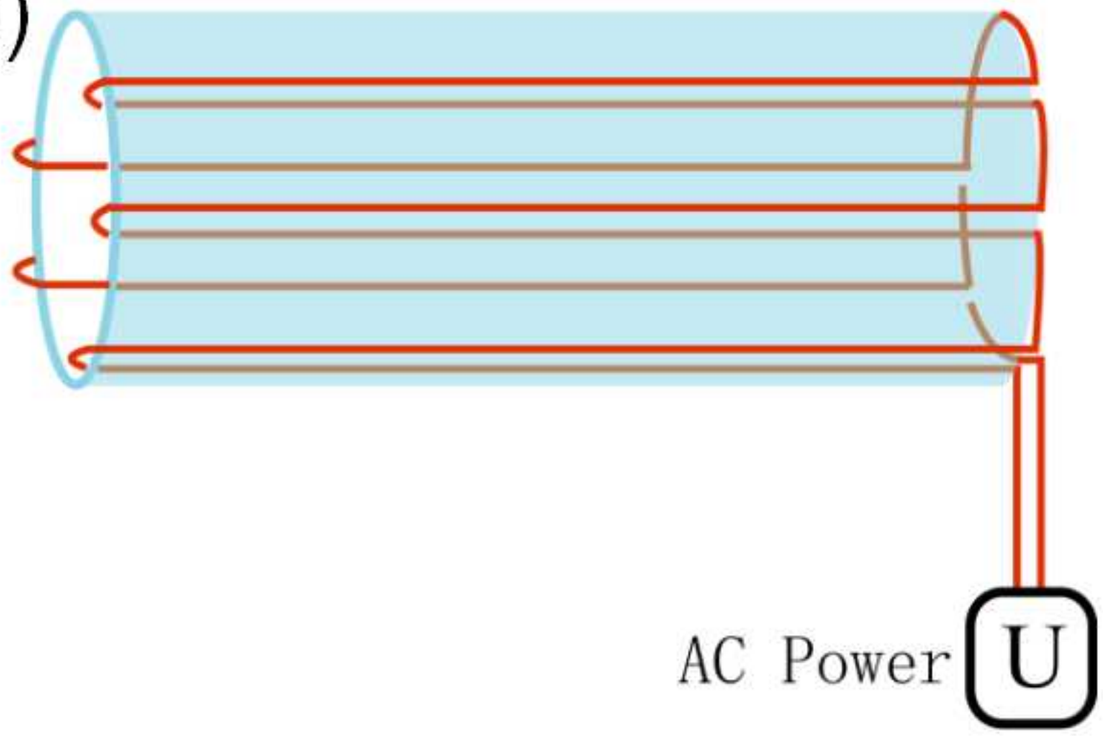
AC Power
U

(c)

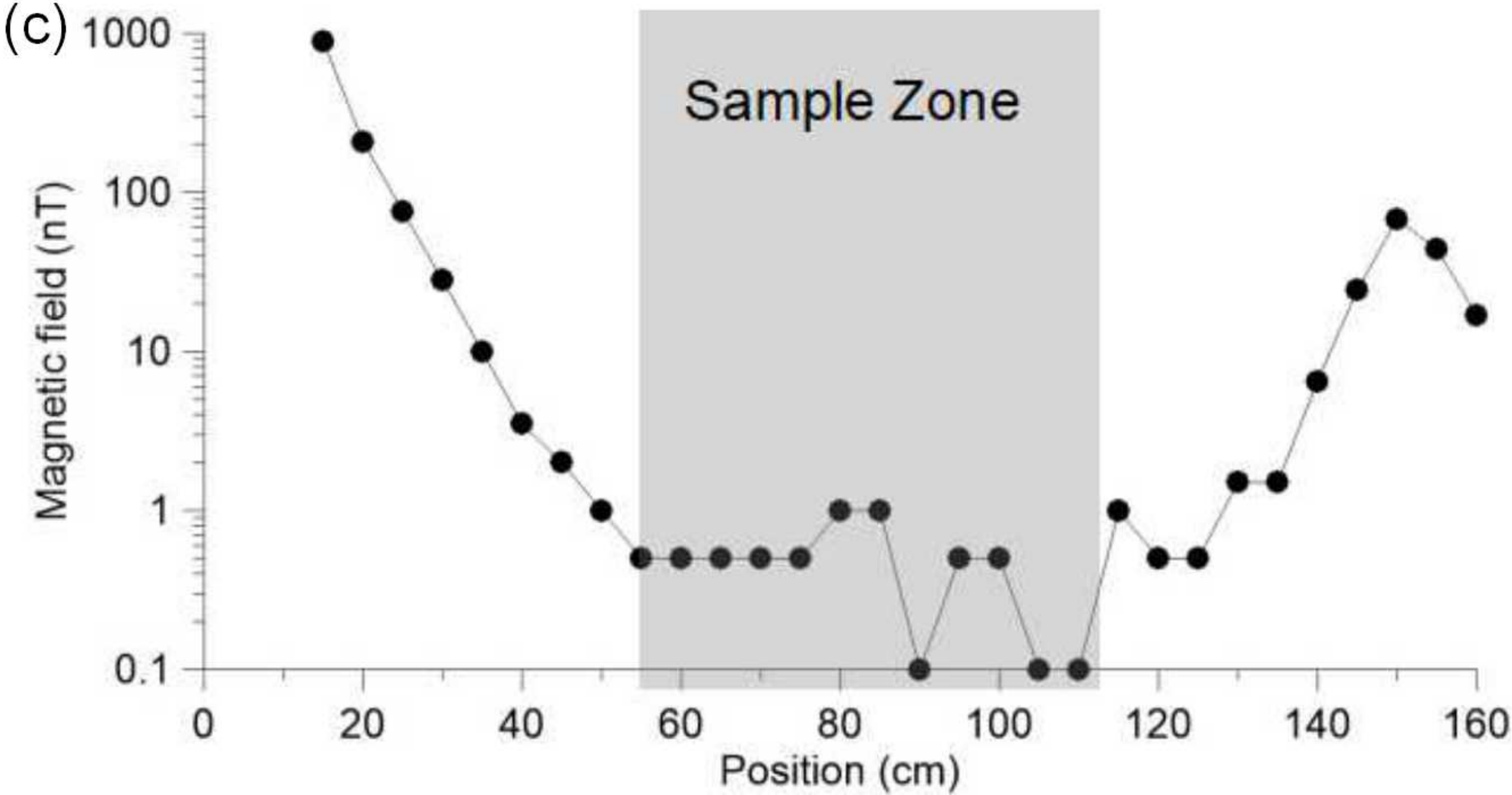
Sample Zone
Magnetic field (nT)
1000
100
10
1
0.1
0
20
40
60
80
100
120
140
160
Position (cm)

Figure 2.

(a)

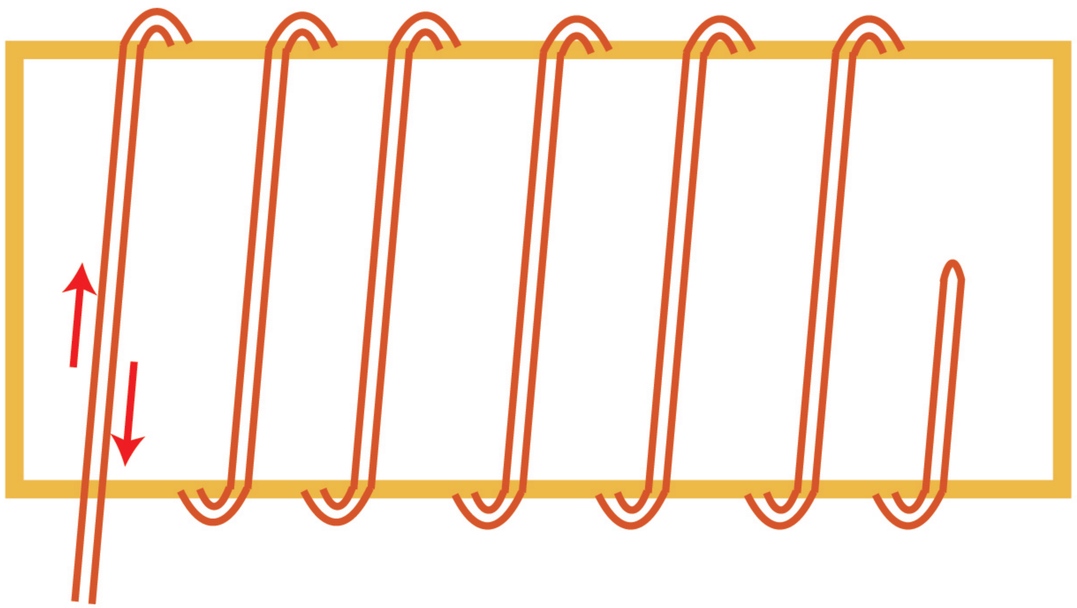

(b)

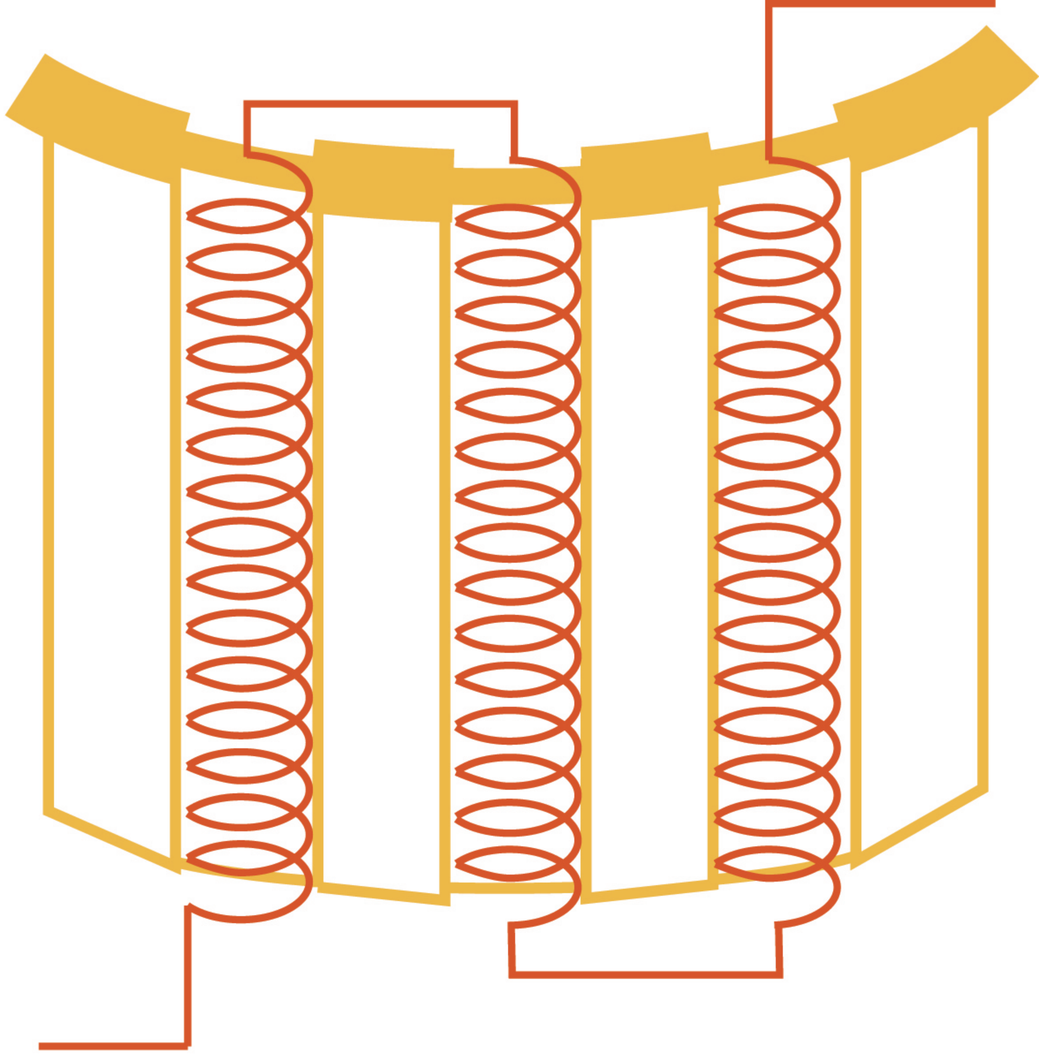

(c)

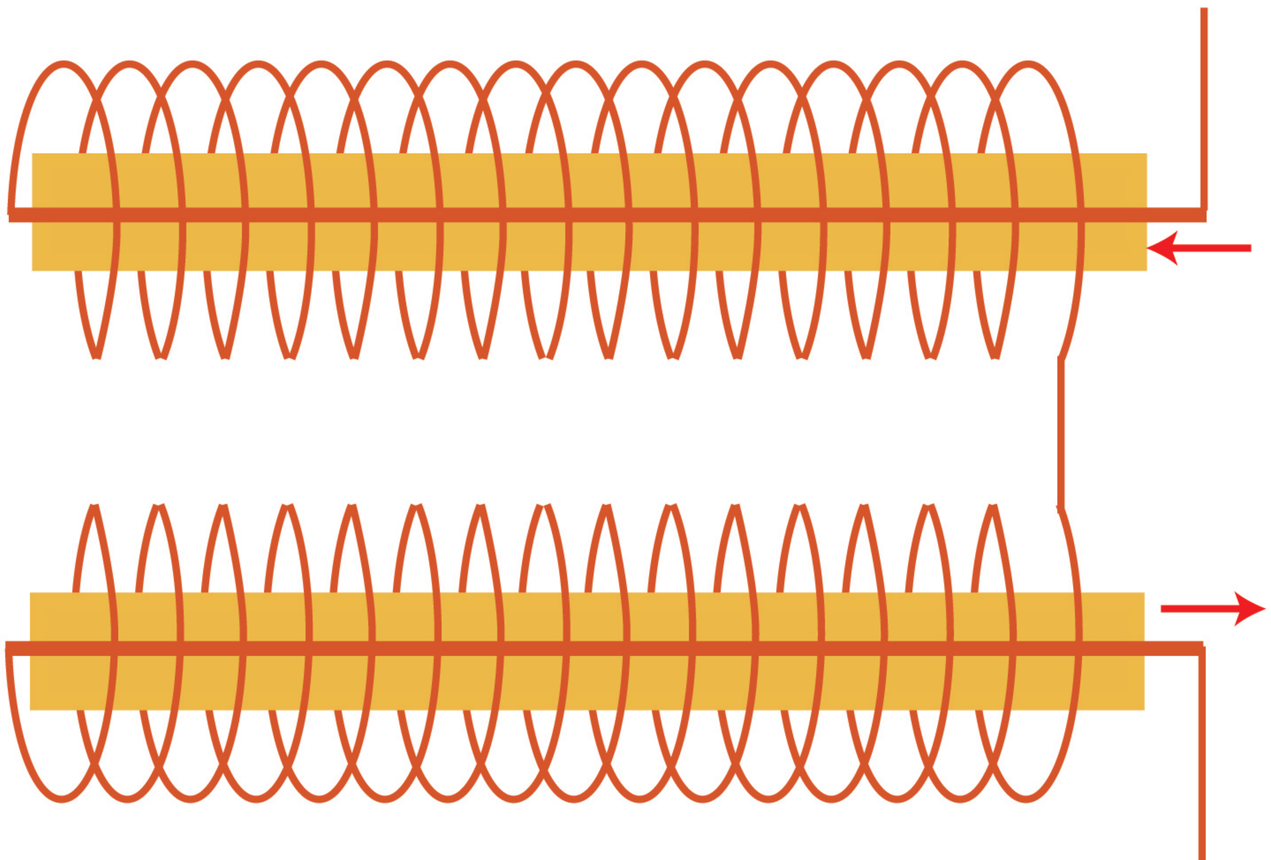

Figure 3.

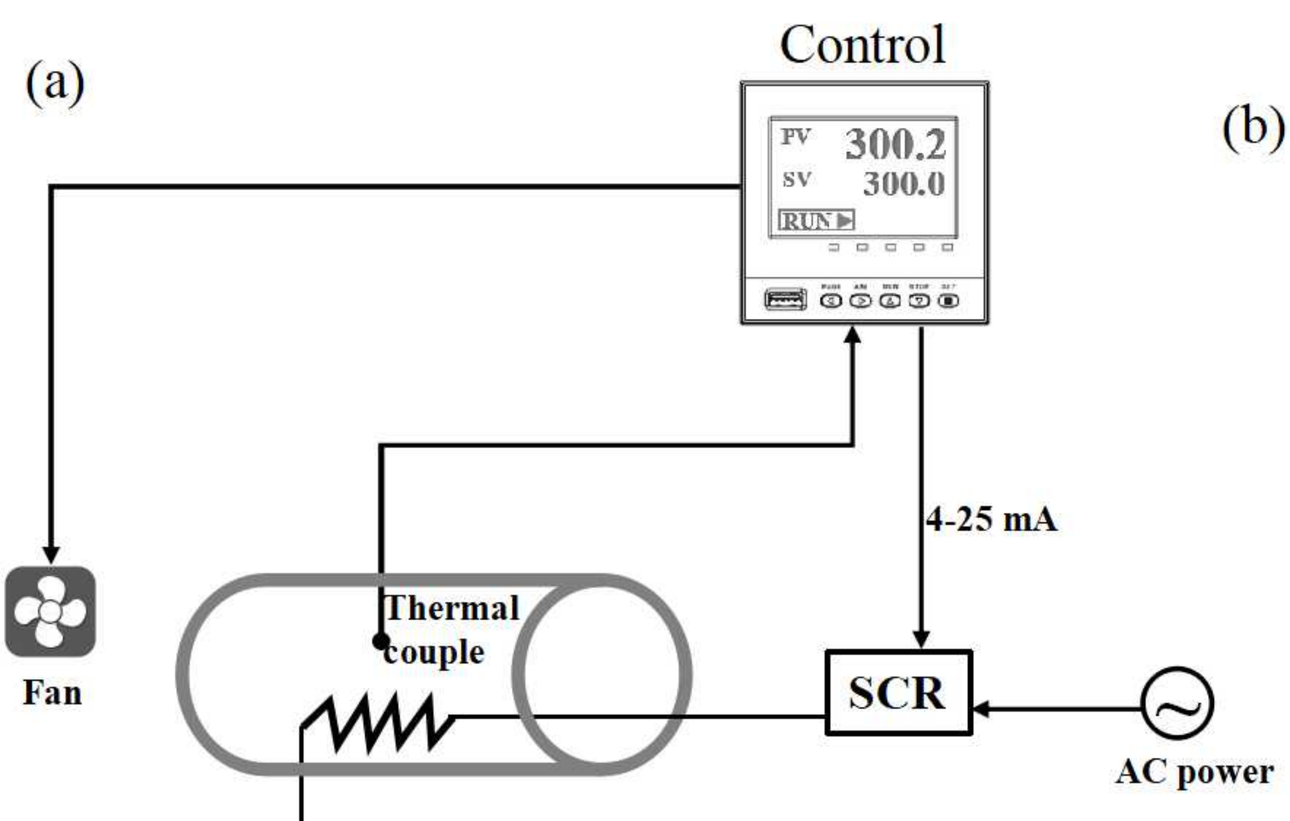
(a)
Control
PV
300.2
SV
300.0
RUN
4-25 mA
Thermal couple
Fan
SCR
AC power

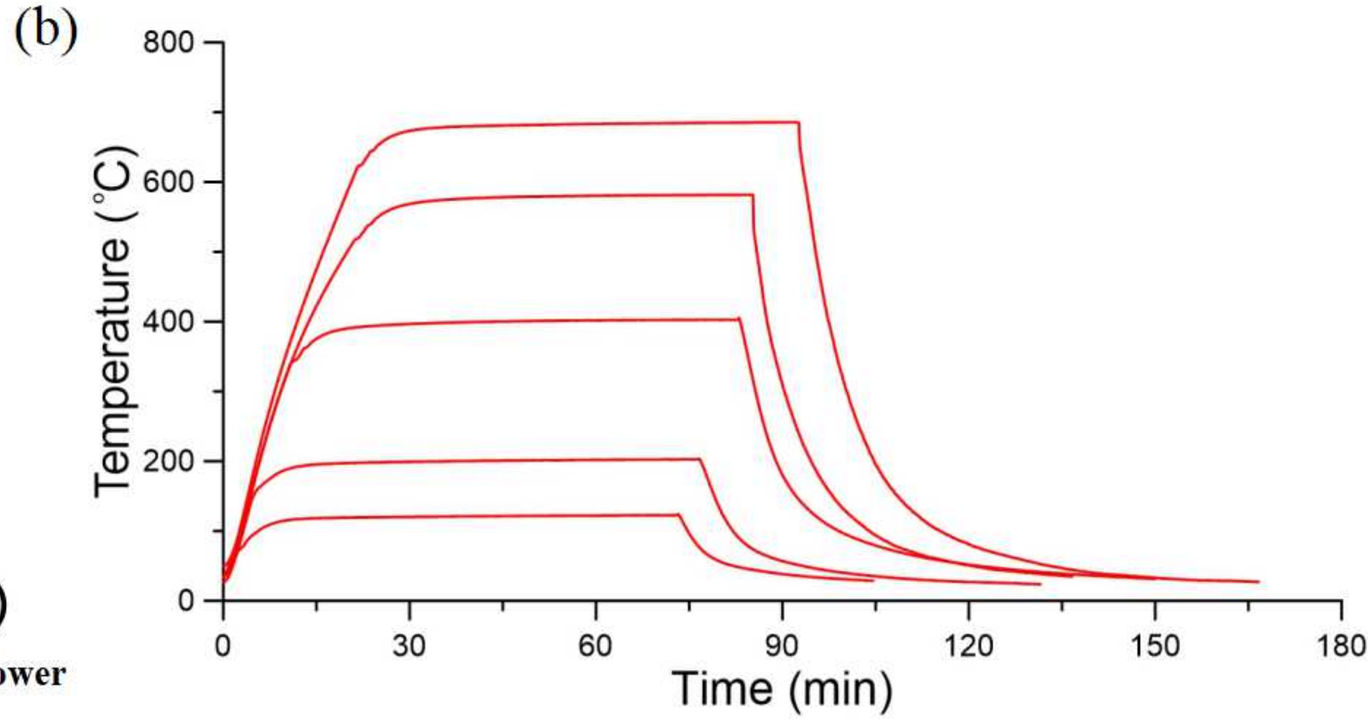
(b)
Temperature (°C)
Time (min)
0
200
400
600
800
0
30
60
90
120
150
180

Figure 4.

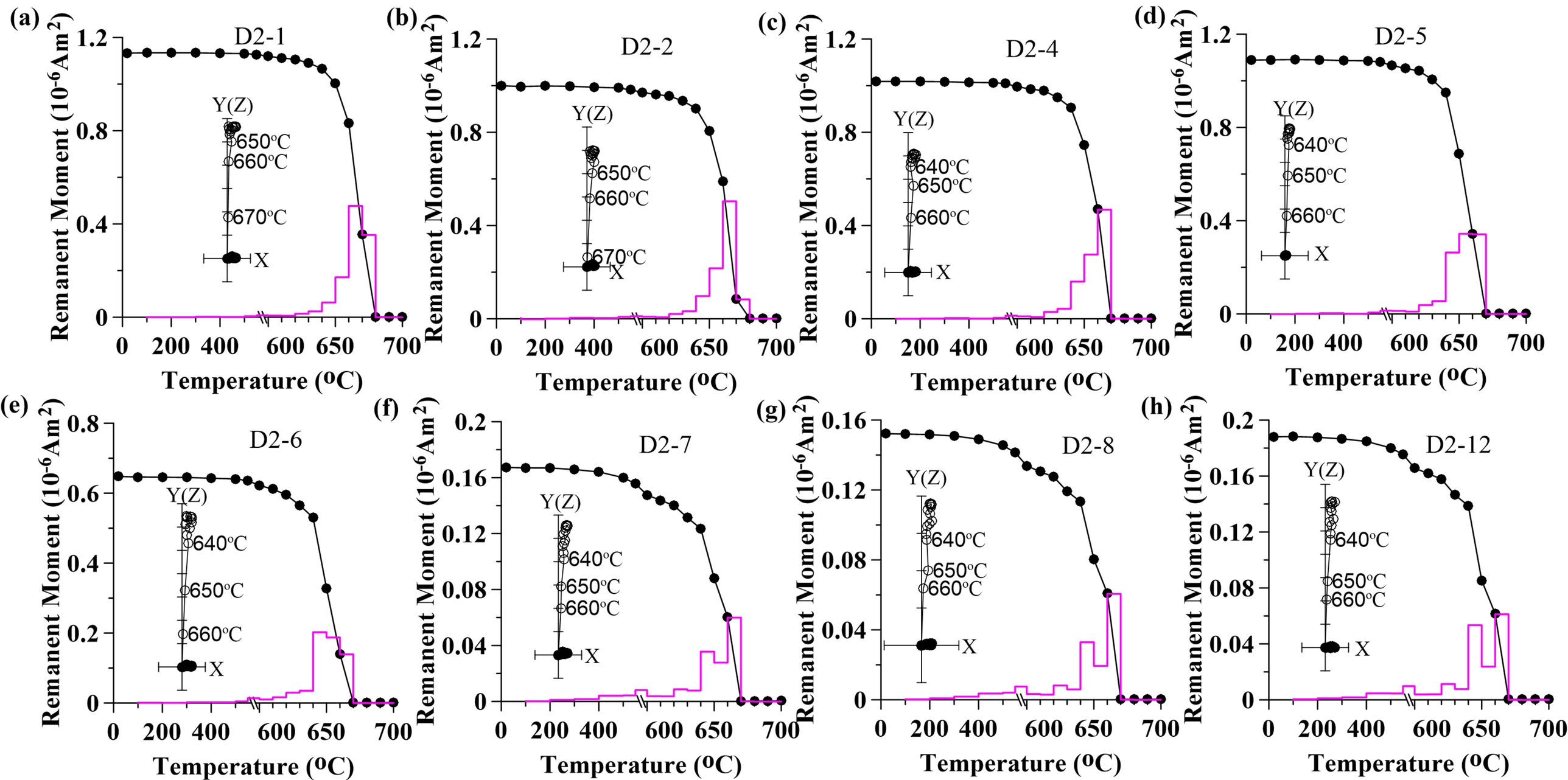
(a)
D2-1
Y(Z)
650°C
660°C
670°C
X
(b)
D2-2
Y(Z)
650°C
660°C
670°C
X
(c)
D2-4
Y(Z)
640°C
650°C
660°C
X
(d)
D2-5
Y(Z)
640°C
650°C
660°C
X
(e)
D2-6
Y(Z)
640°C
650°C
660°C
X
(f)
D2-7
Y(Z)
640°C
650°C
660°C
X
(g)
D2-8
Y(Z)
640°C
650°C
660°C
X
(h)
D2-12
Y(Z)
640°C
650°C
660°C
X
Remanent Moment (10^{-6}Am^2)
Temperature (°C)
0
200
400
600
650
700

Figure 5.

(a)

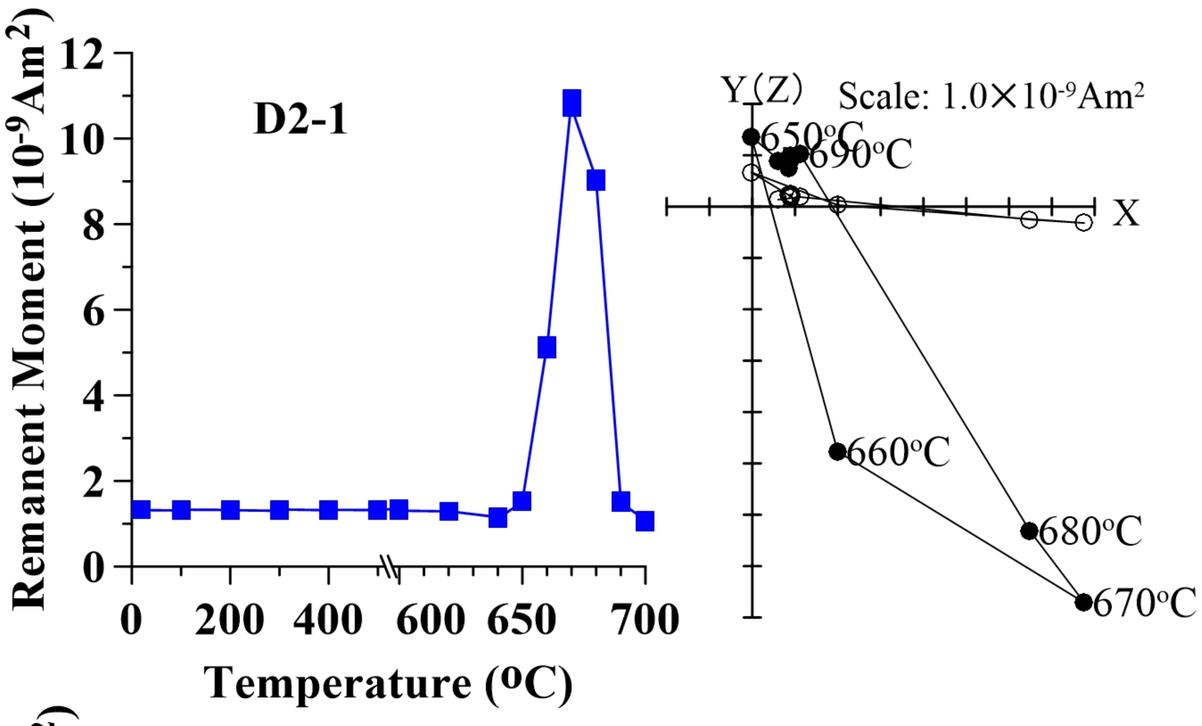
D2-1
Remanent Moment (10-9Am2)
Temperature (oC)
Y(Z)
Scale: 1.0×10-9Am2
X
650oC
690oC
660oC
680oC
670oC

(b)

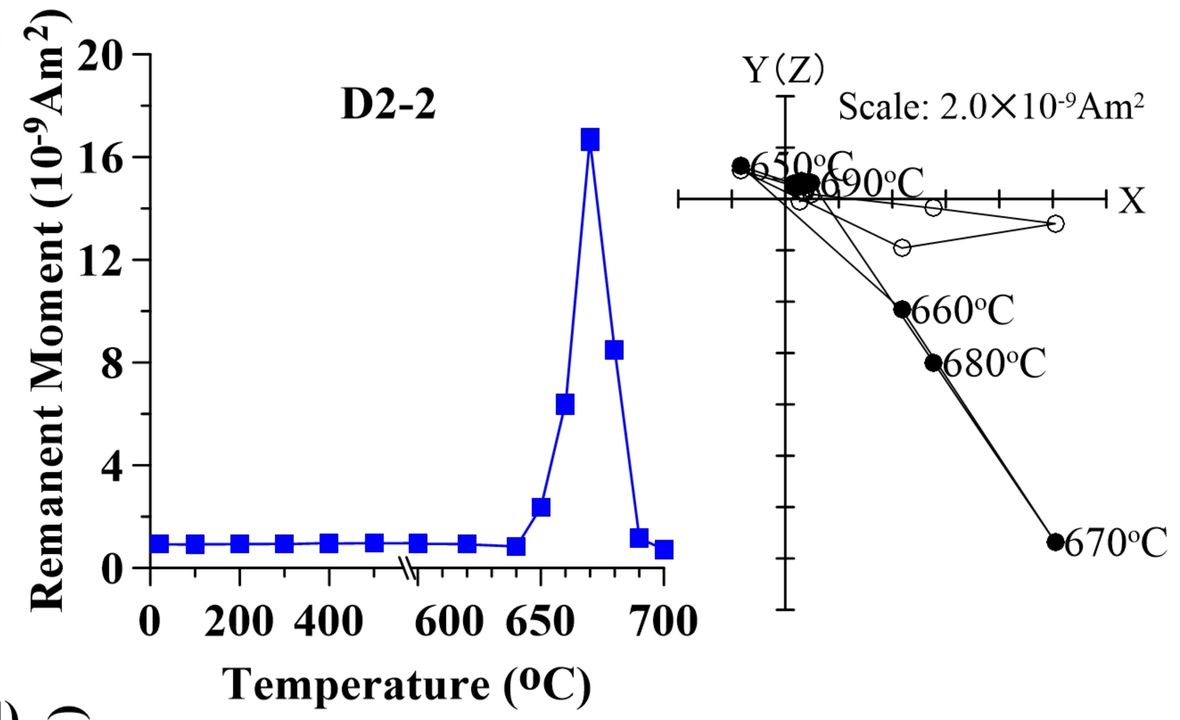
D2-2
Remanent Moment (10-9Am2)
Temperature (oC)
Y(Z)
Scale: 2.0×10-9Am2
X
650oC
690oC
660oC
680oC
670oC

(c)

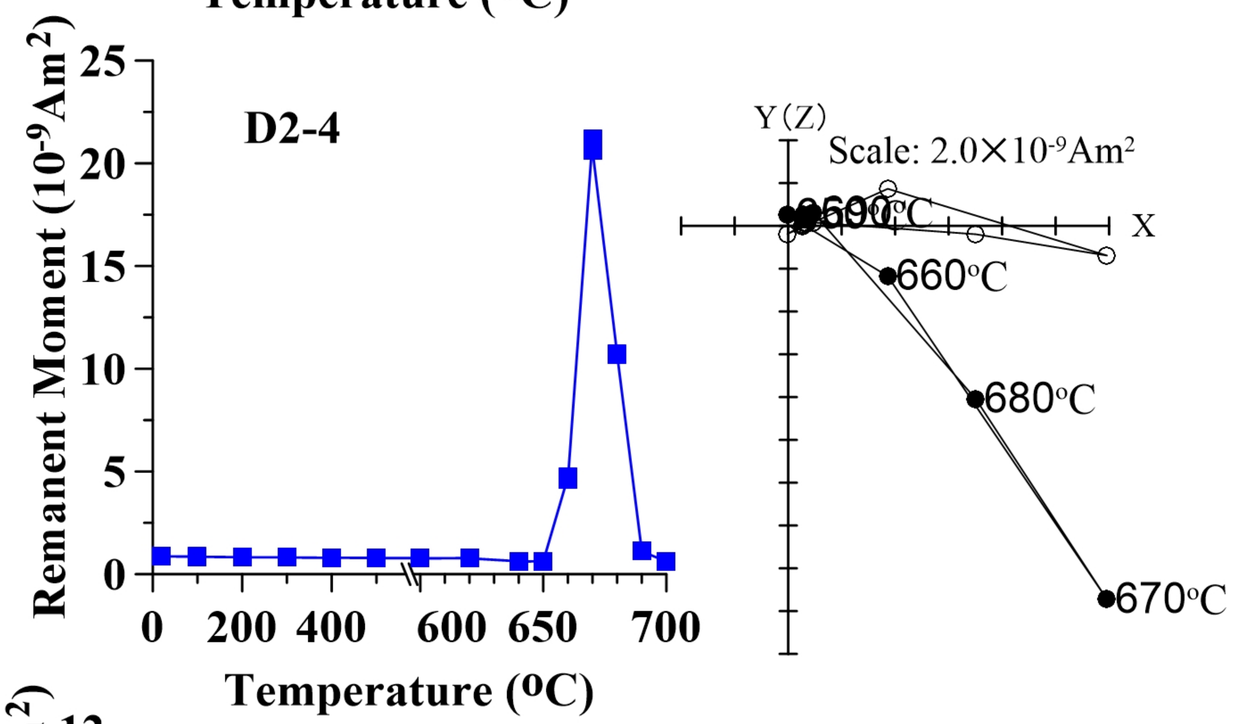
D2-4
Remanent Moment (10-9Am2)
Temperature (oC)
Y(Z)
Scale: 2.0×10-9Am2
X
690oC
660oC
680oC
670oC

(d)

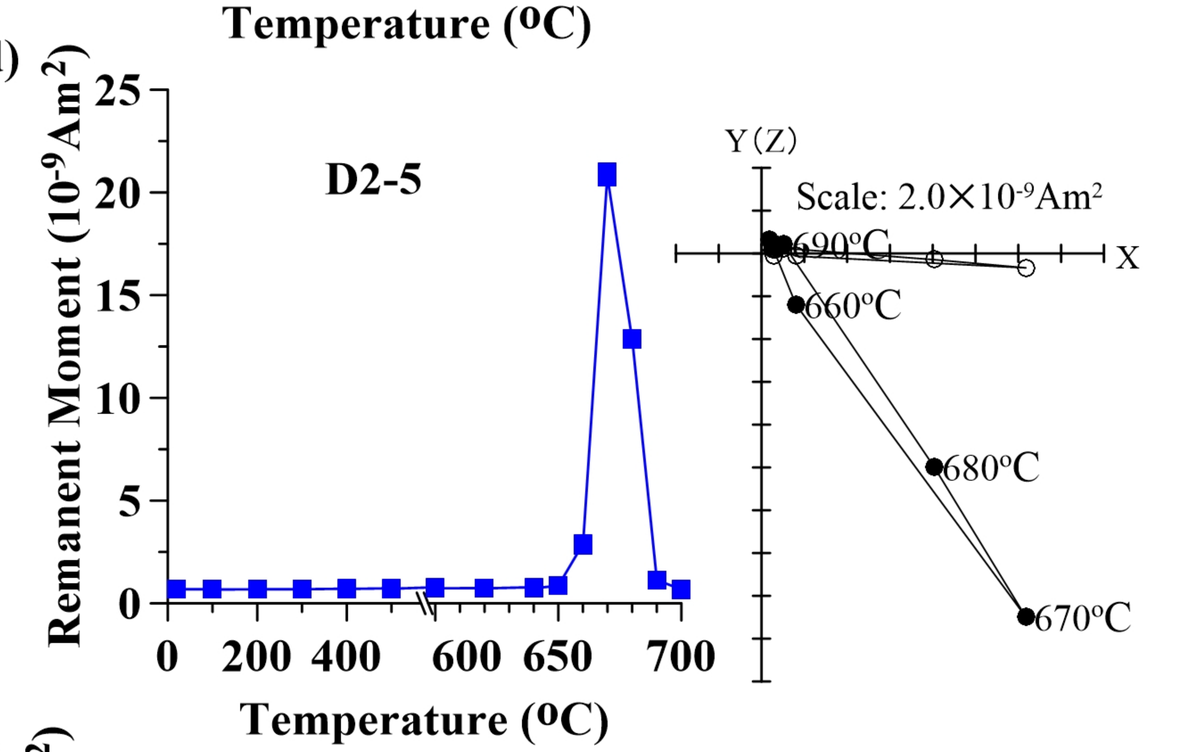
D2-5
Remanent Moment (10-9Am2)
Temperature (oC)
Y(Z)
Scale: 2.0×10-9Am2
X
690oC
660oC
680oC
670oC

(e)

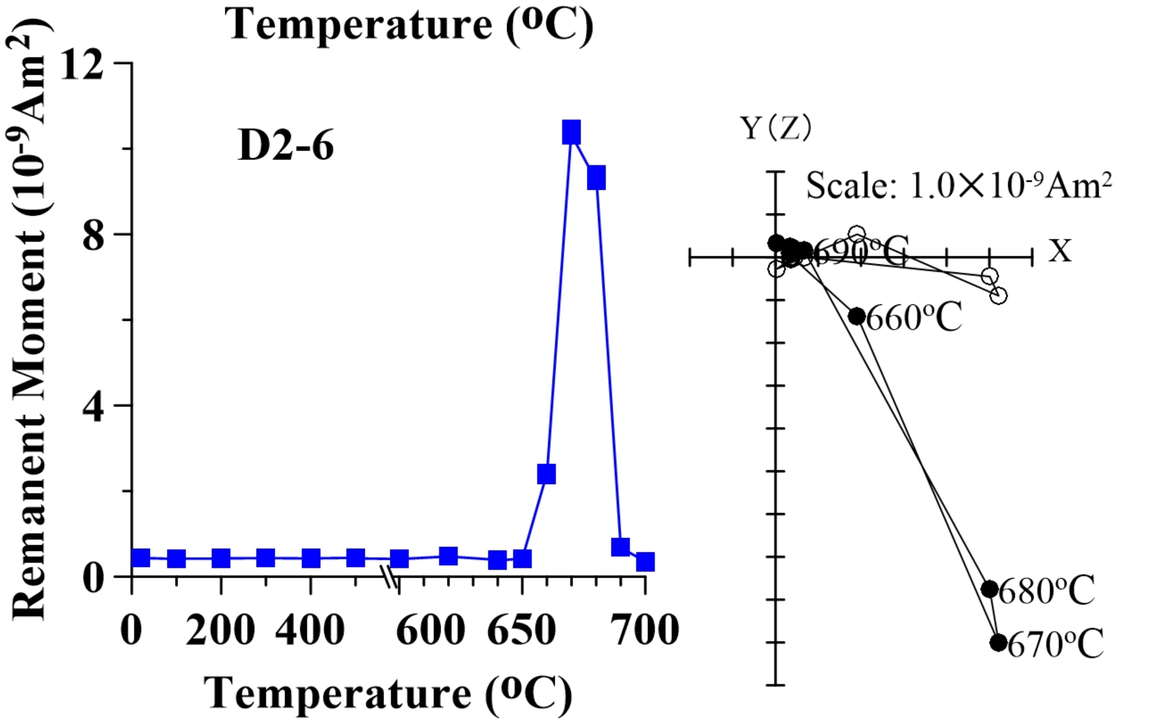
D2-6
Remanent Moment (10-9Am2)
Temperature (oC)
Y(Z)
Scale: 1.0×10-9Am2
X
690oC
660oC
680oC
670oC

(f)

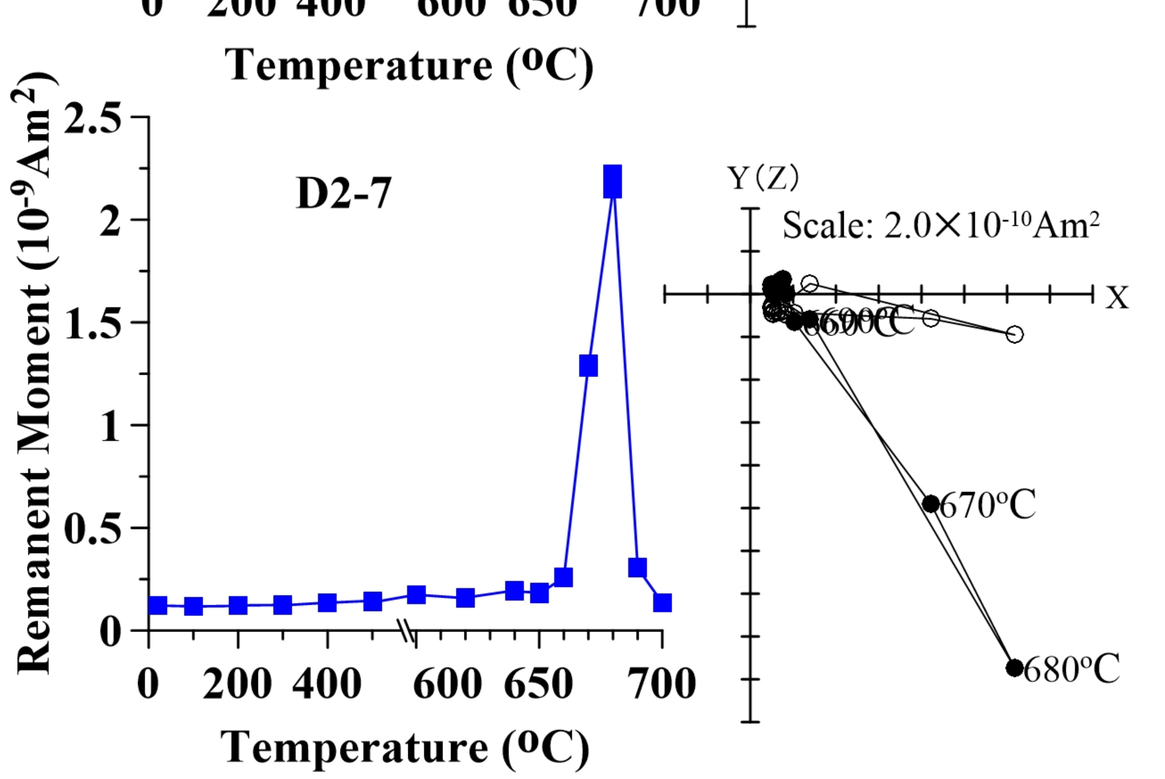
D2-7
Remanent Moment (10-9Am2)
Temperature (oC)
Y(Z)
Scale: 2.0×10-10Am2
X
660oC
670oC
680oC

(g)

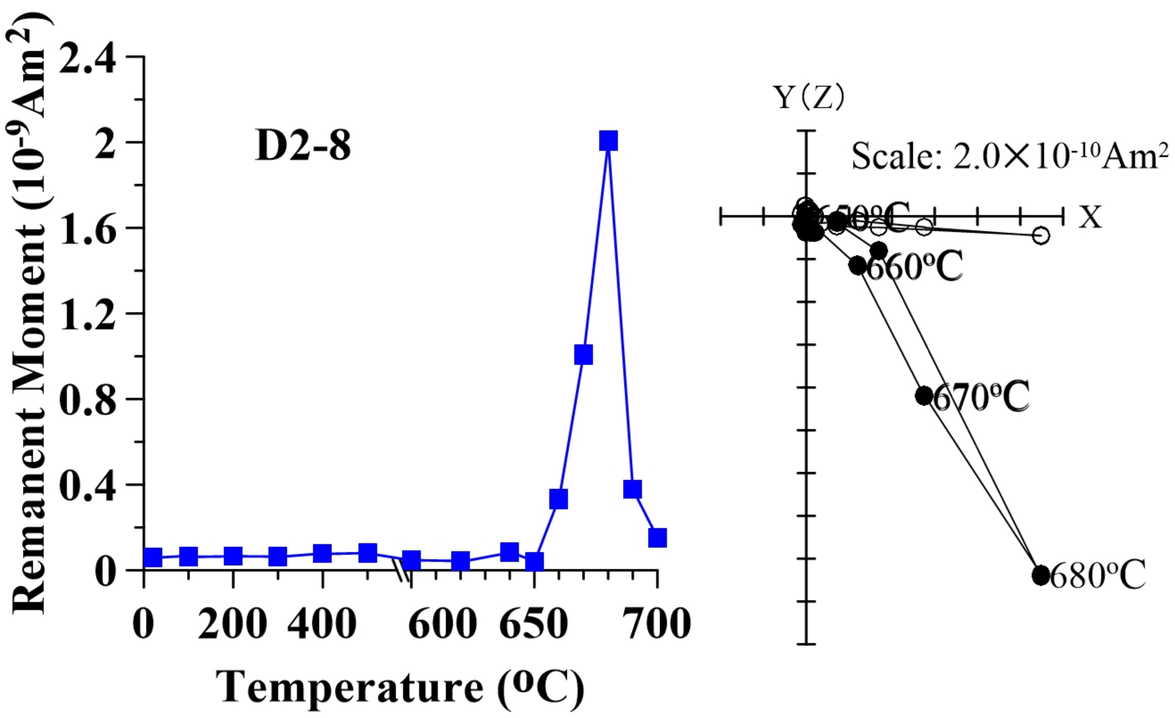
D2-8
Remanent Moment (10-9Am2)
Temperature (oC)
Y(Z)
Scale: 2.0×10-10Am2
X
660oC
670oC
680oC

(h)

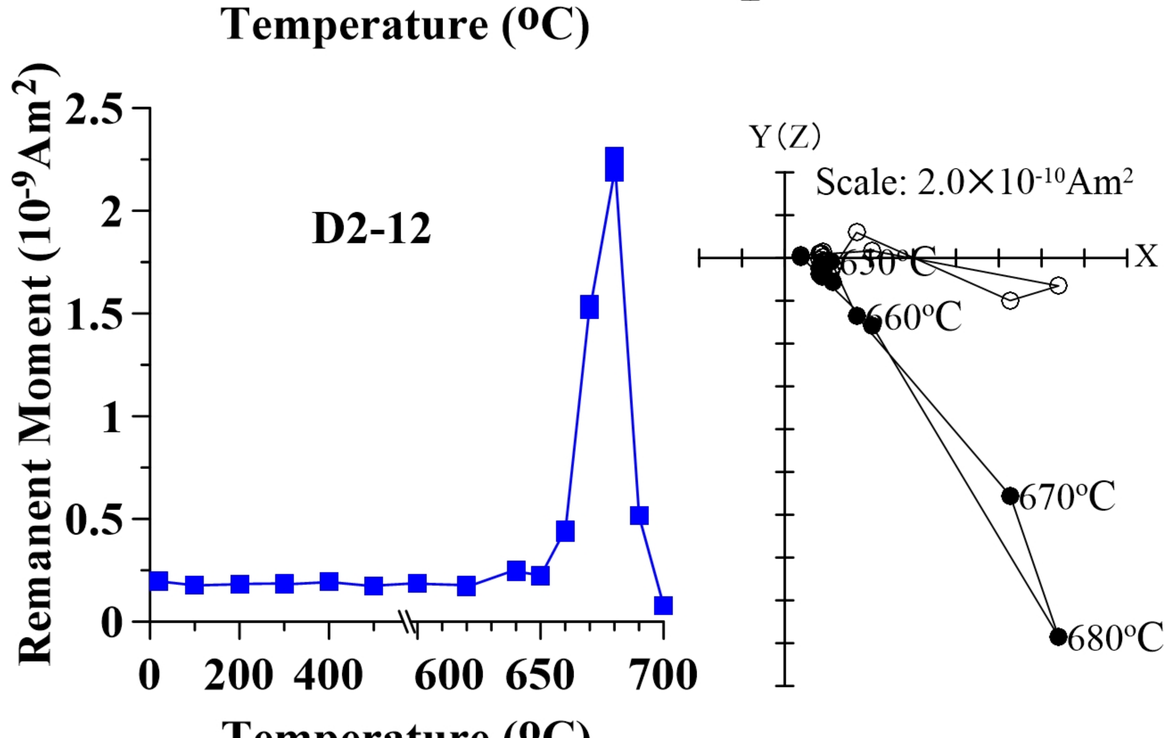
D2-12
Remanent Moment (10-9Am2)
Temperature (oC)
Y(Z)
Scale: 2.0×10-10Am2
X
660oC
670oC
680oC

Figure 6.

(a)

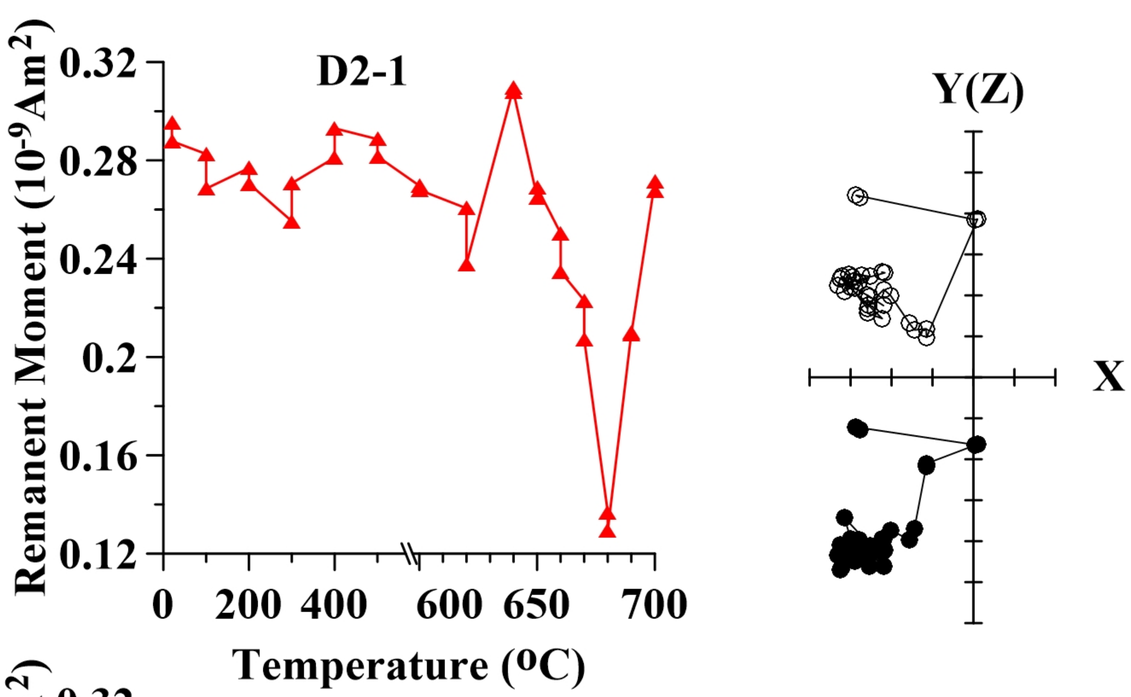
D2-1
Remanent Moment (10^{-9}Am^2)
0.32
0.28
0.24
0.2
0.16
0.12
0
200
400
600
650
700
Temperature (^{o}C)
Y(Z)
X

(b)

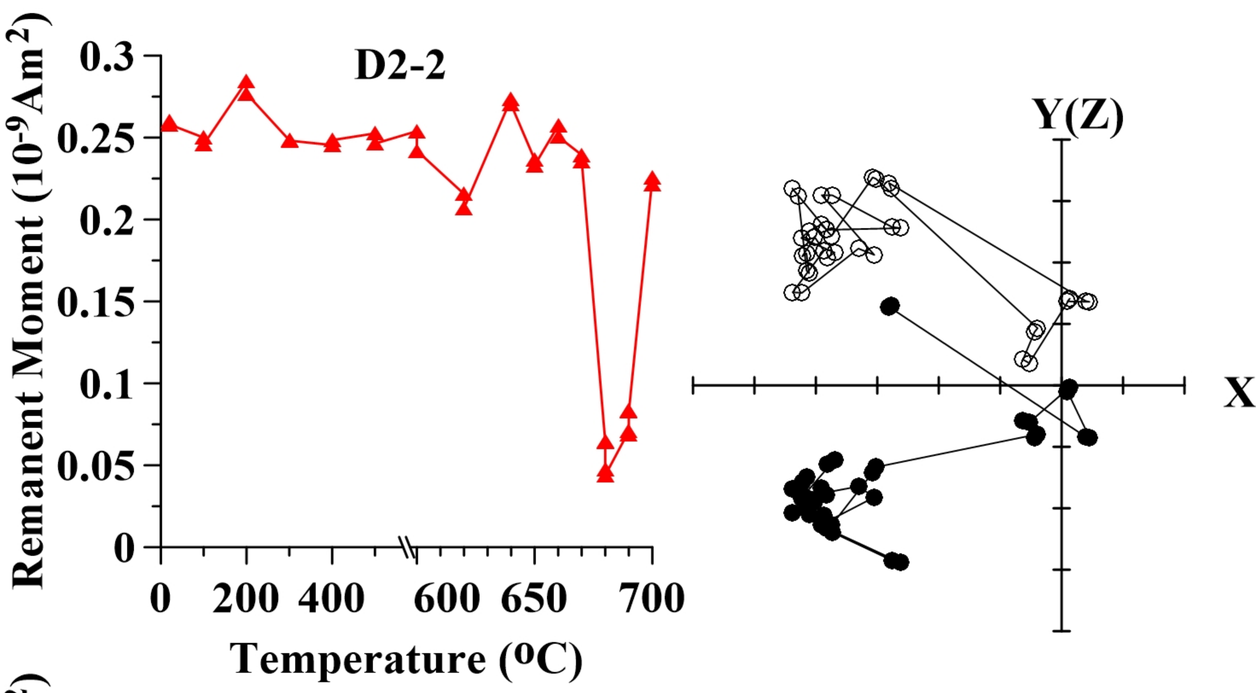
D2-2
Remanent Moment (10^{-9}Am^2)
0.3
0.25
0.2
0.15
0.1
0.05
0
0
200
400
600
650
700
Temperature (^{o}C)
Y(Z)
X

(c)

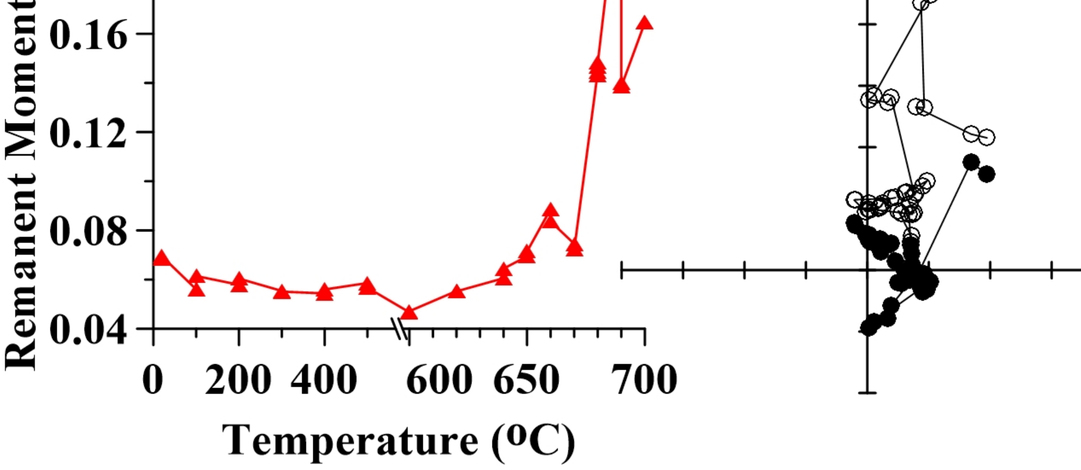
D2-4
Remanent Moment (10^{-9}Am^2)
0.32
0.28
0.24
0.2
0.16
0.12
0
200
400
600
650
700
Temperature (^{o}C)
Y(Z)
X

(d)

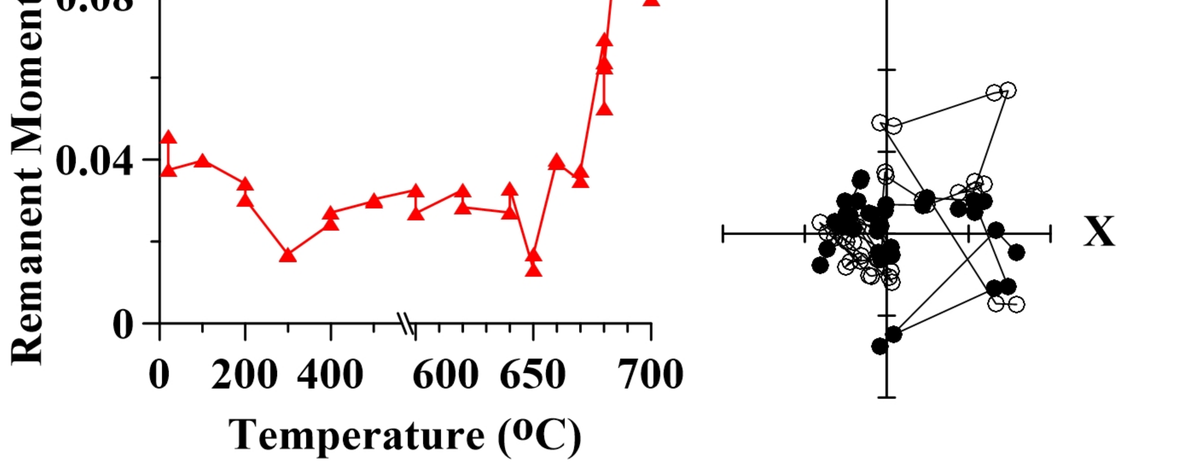
D2-5
Remanent Moment (10^{-9}Am^2)
0.36
0.32
0.28
0.24
0.2
0.16
0
200
400
600
650
700
Temperature (^{o}C)
Y(Z)
X

(e)

D2-6
Remanent Moment (10^{-9}Am^2)
0.24
0.2
0.16
0.12
0.08
0.04
0
200
400
600
650
700
Temperature (^{o}C)
Y(Z)
X

(f)

D2-7
Remanent Moment (10^{-9}Am^2)
0.12
0.08
0.04
0
0
200
400
600
650
700
Temperature (^{o}C)
Y(Z)
X

(g)

D2-8
Remanent Moment (10^{-9}Am^2)
0.06
0.05
0.04
0.03
0.02
0.01
0
200
400
600
650
700
Temperature (^{o}C)
Y(Z)
X

(h)

D2-12
Remanent Moment (10^{-9}Am^2)
0.14
0.12
0.1
0.08
0.06
0
200
400
600
650
700
Temperature (^{o}C)
Y(Z)
X

Figure 7.

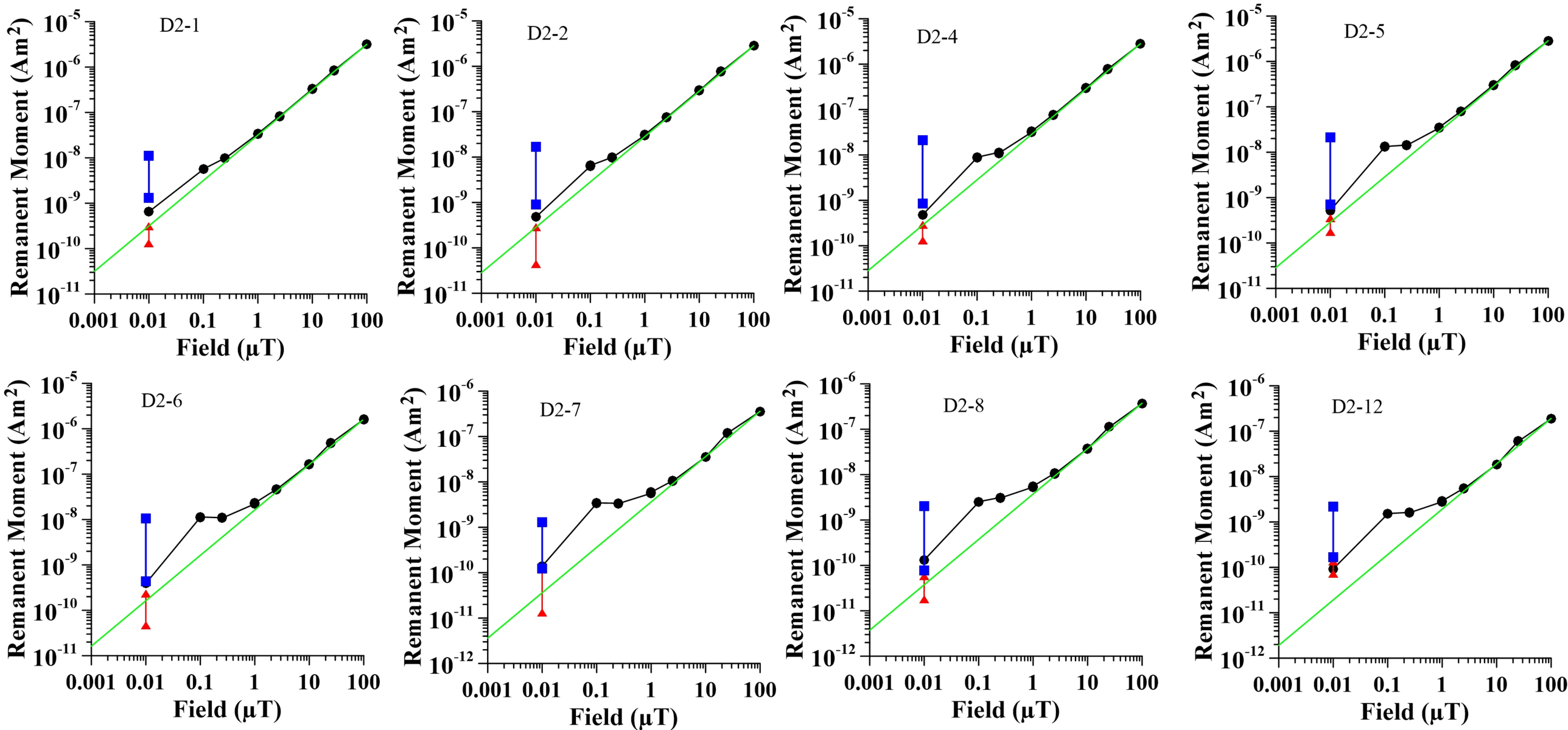
D2-1
D2-2
D2-4
D2-5
D2-6
D2-7
D2-8
D2-12
Remanent Moment (Am²)
Field (μT)
0.001
0.01
0.1
1
10
100

Figure 8.

(a)

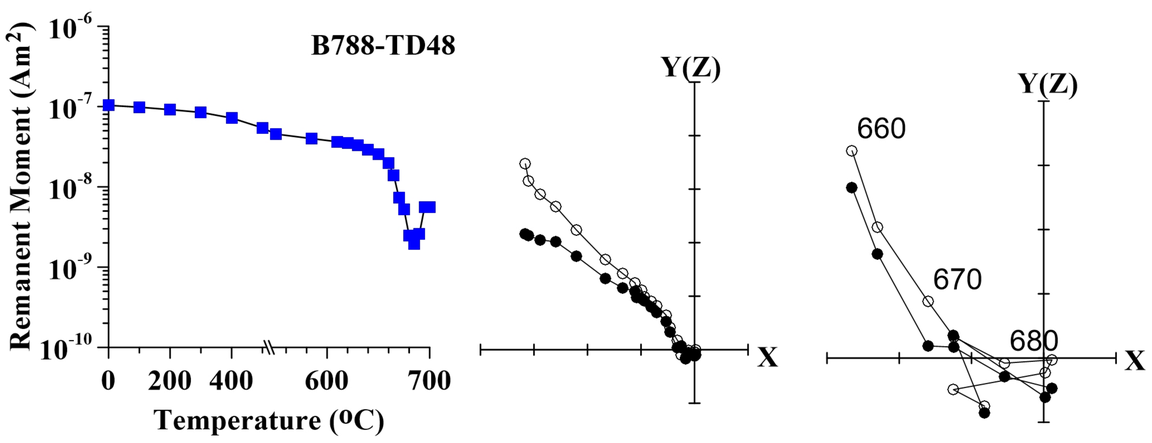

(b)

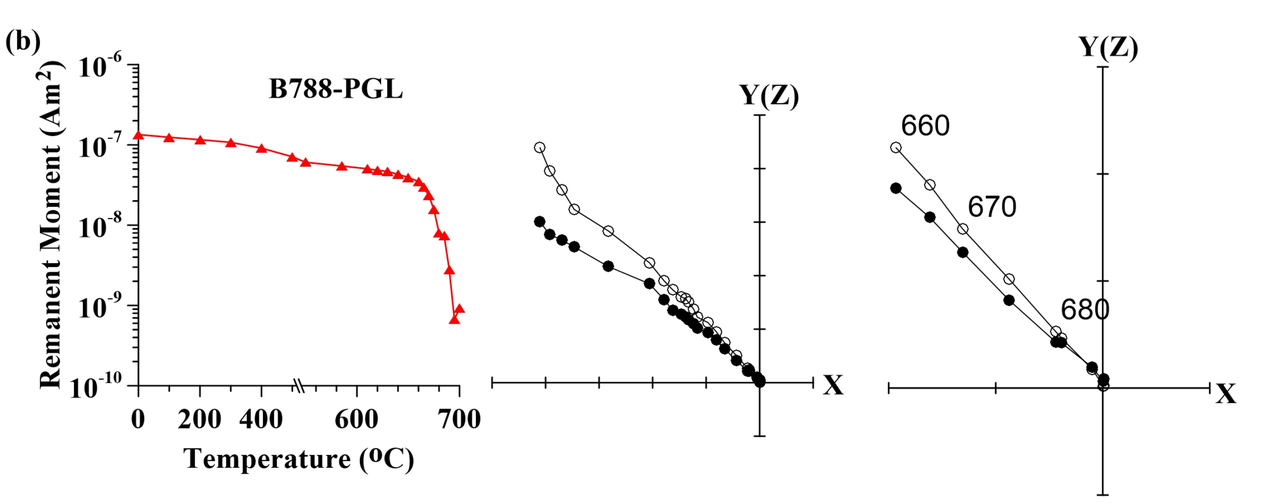

(c)

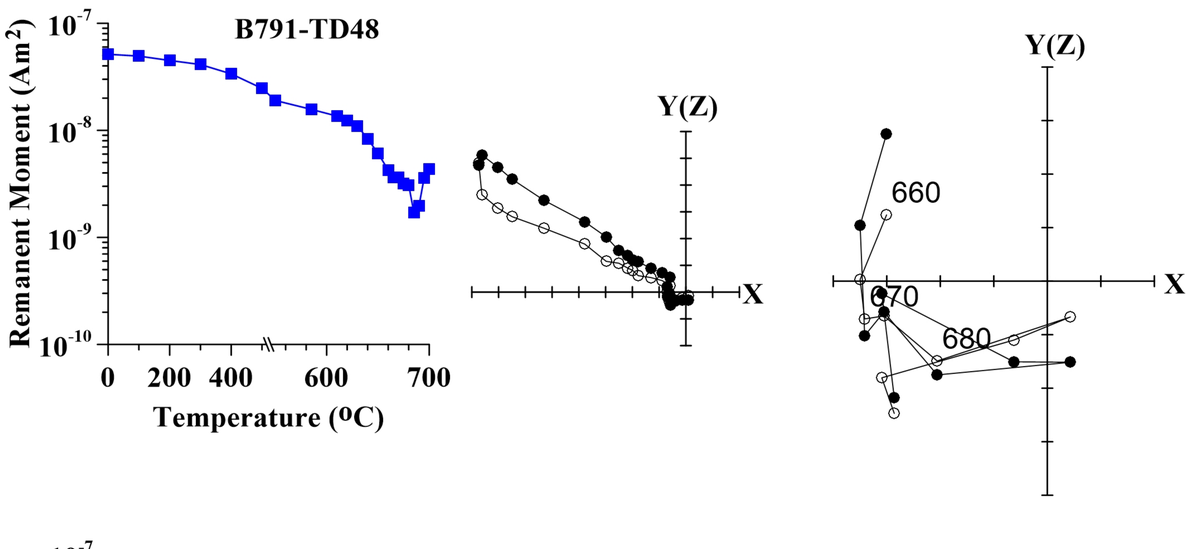

(d)

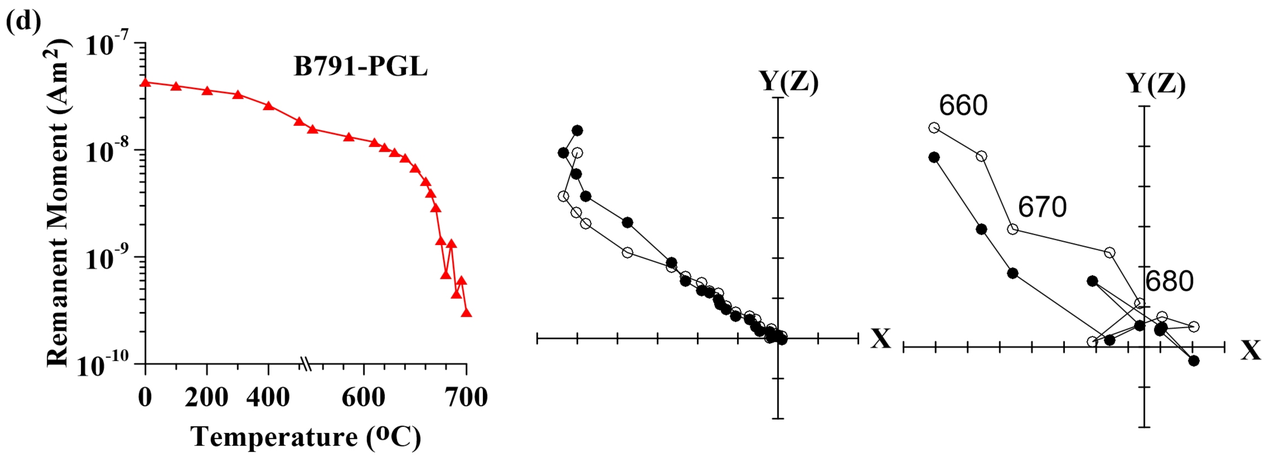

(e)

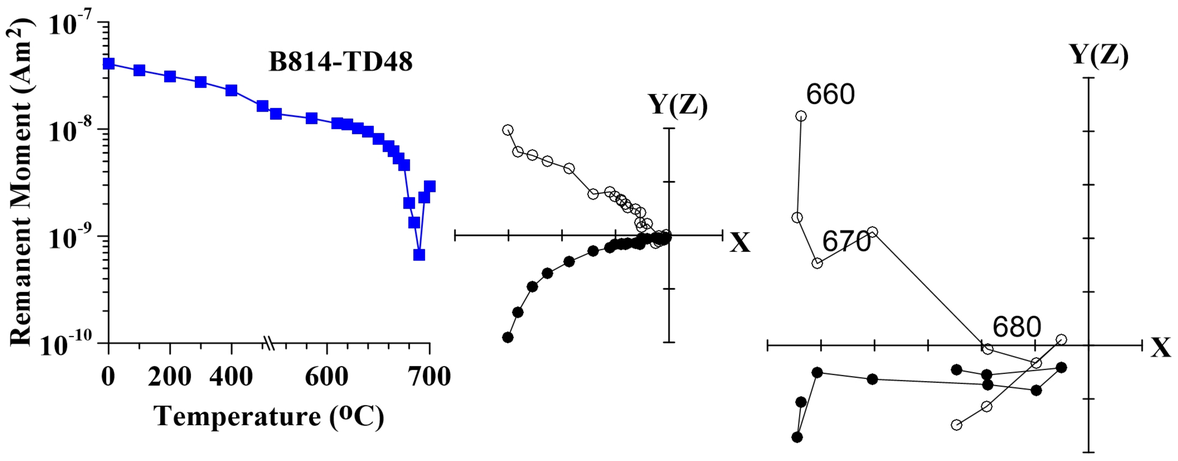

(f)

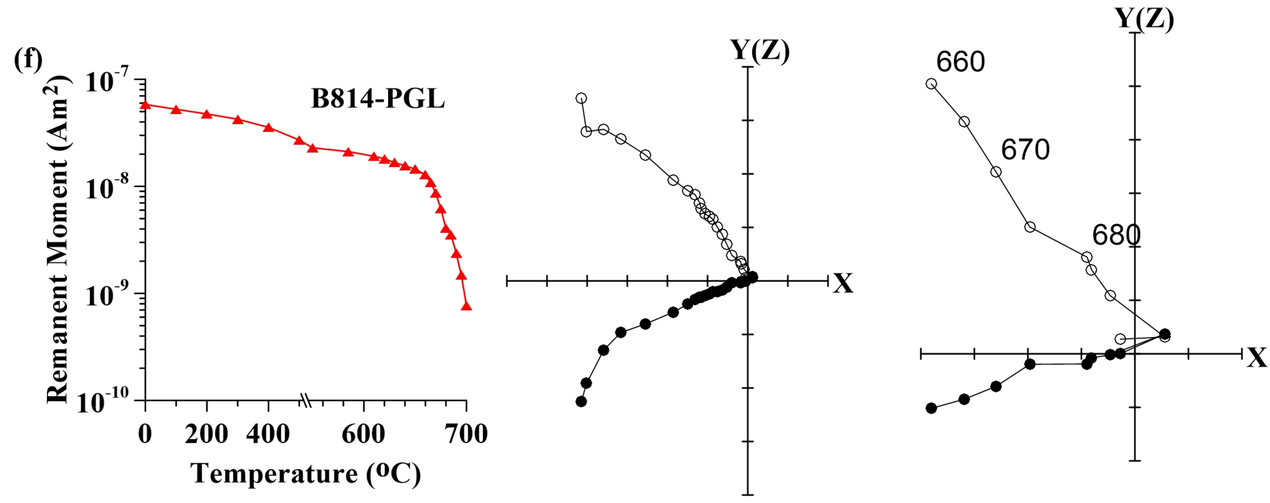

(g)

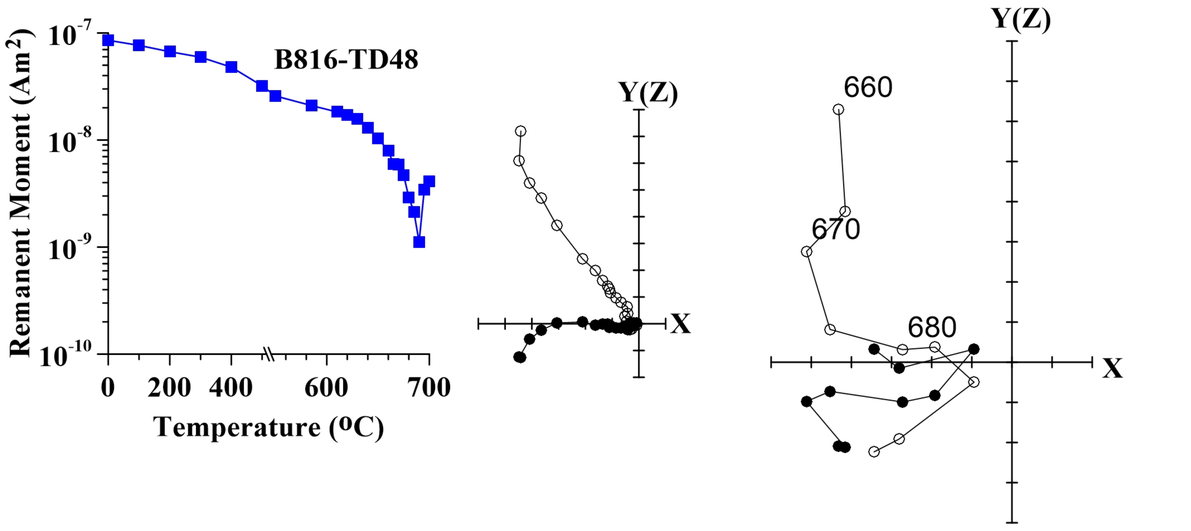

(h)

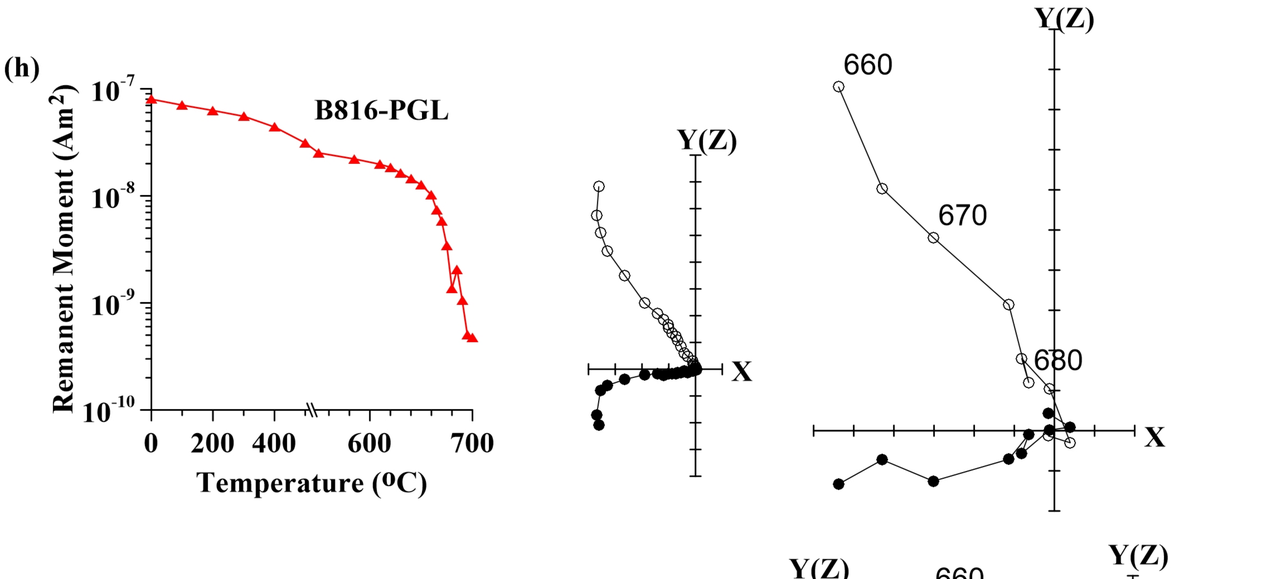

(i)

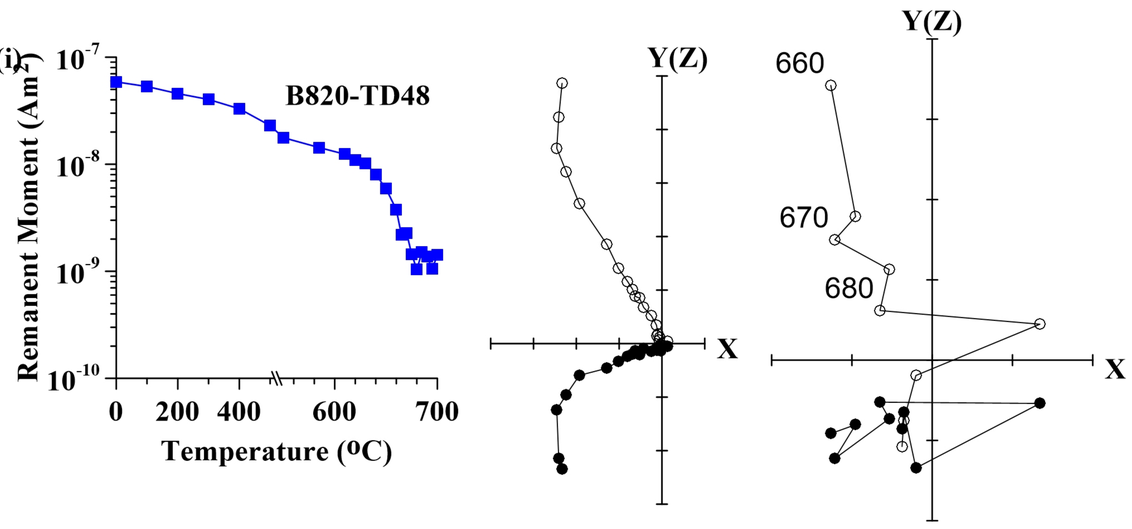

(j)

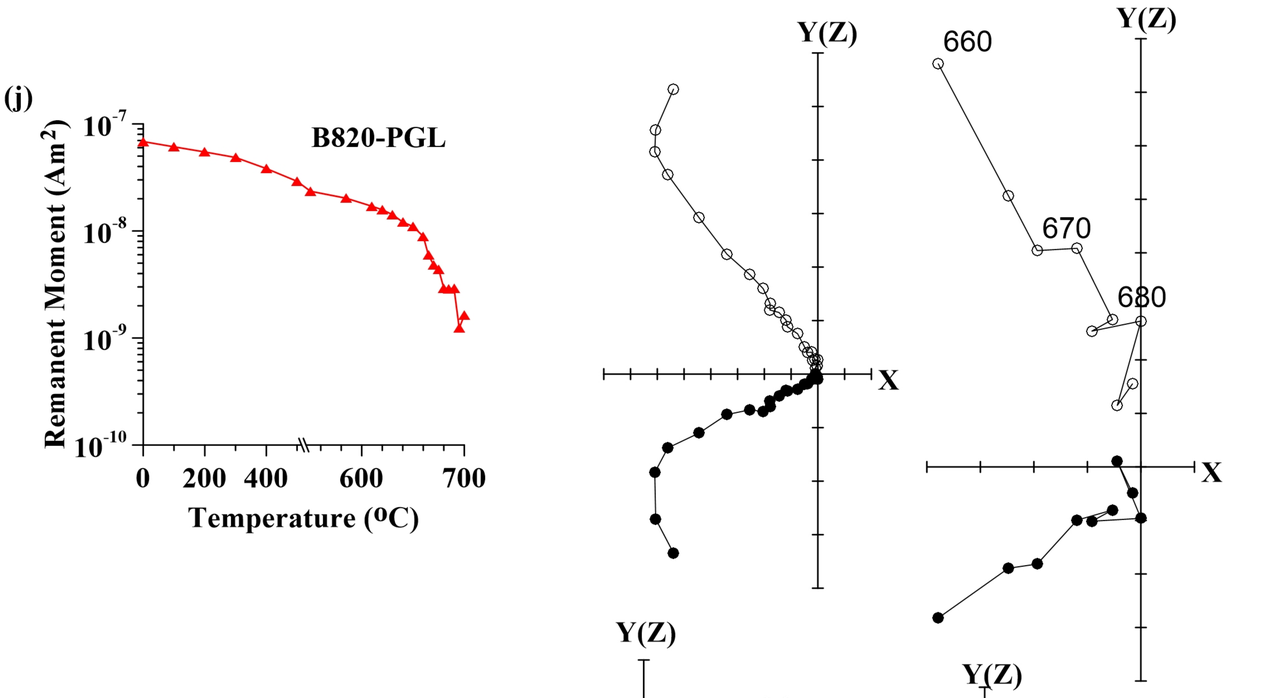

(k)

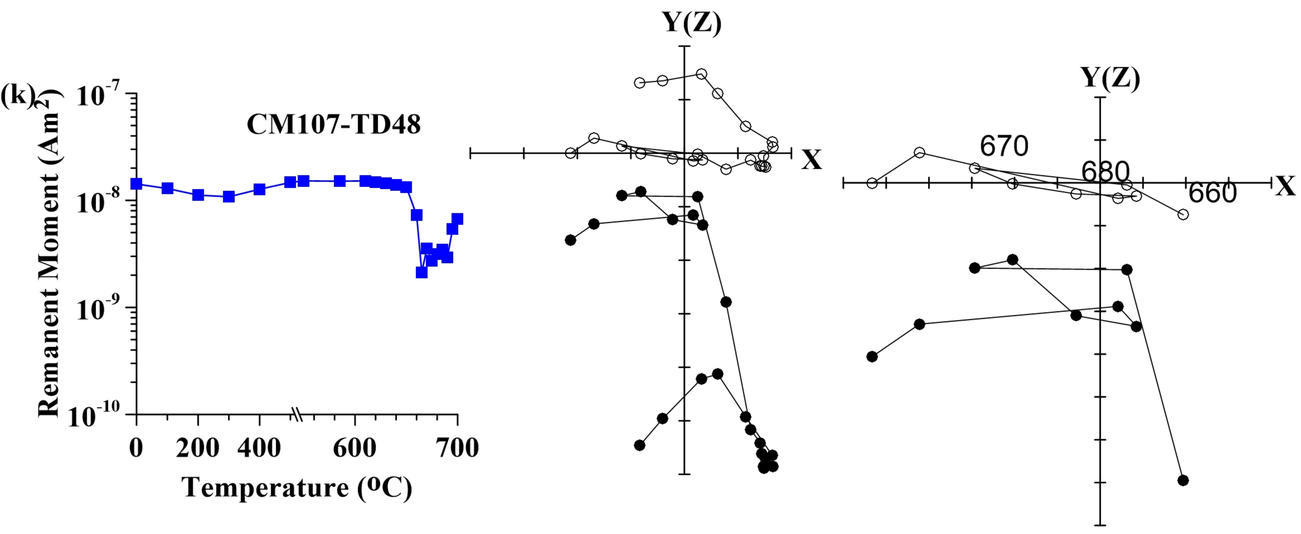

(l)

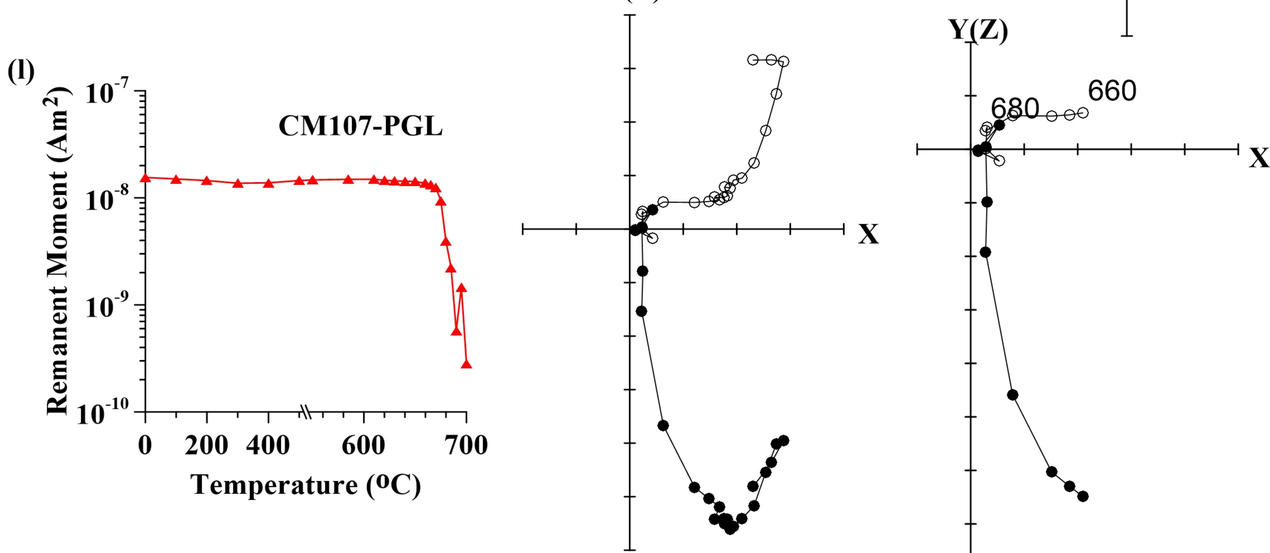

Figure 8(continued).

(m)

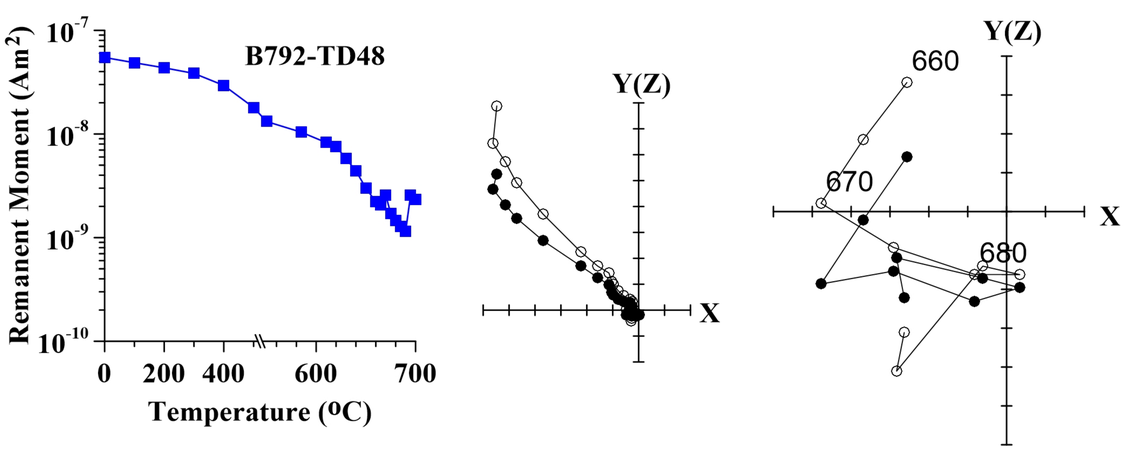

(n)

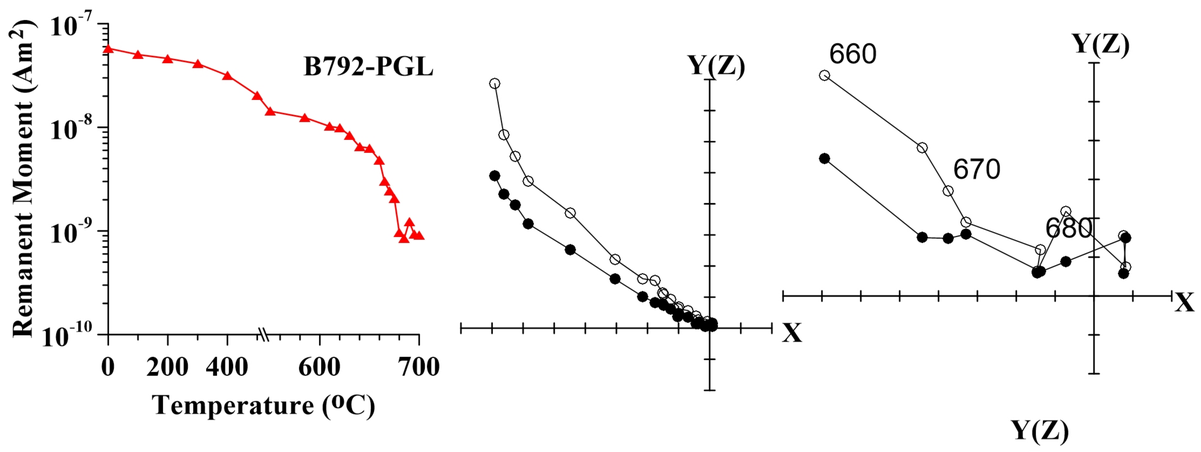

(o)

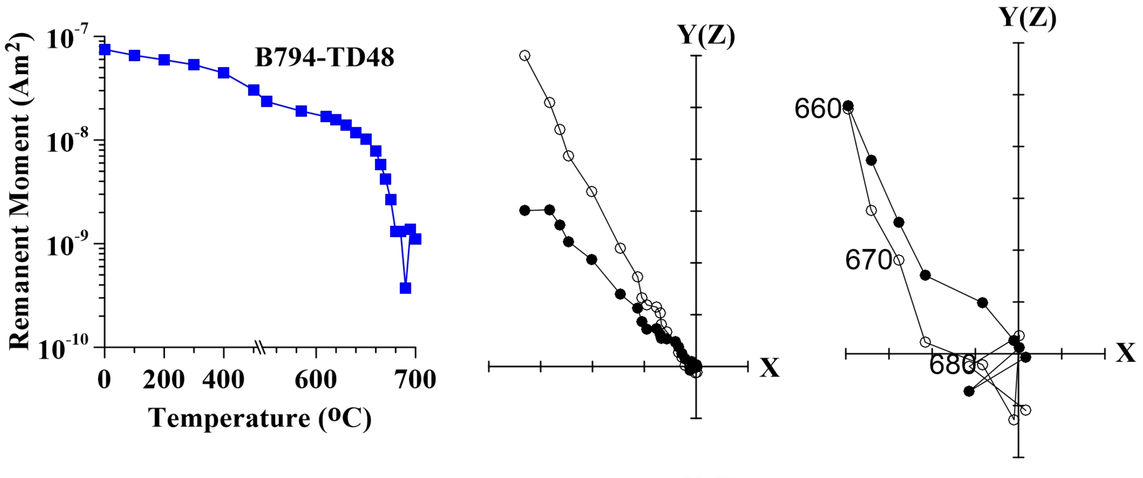

(p)

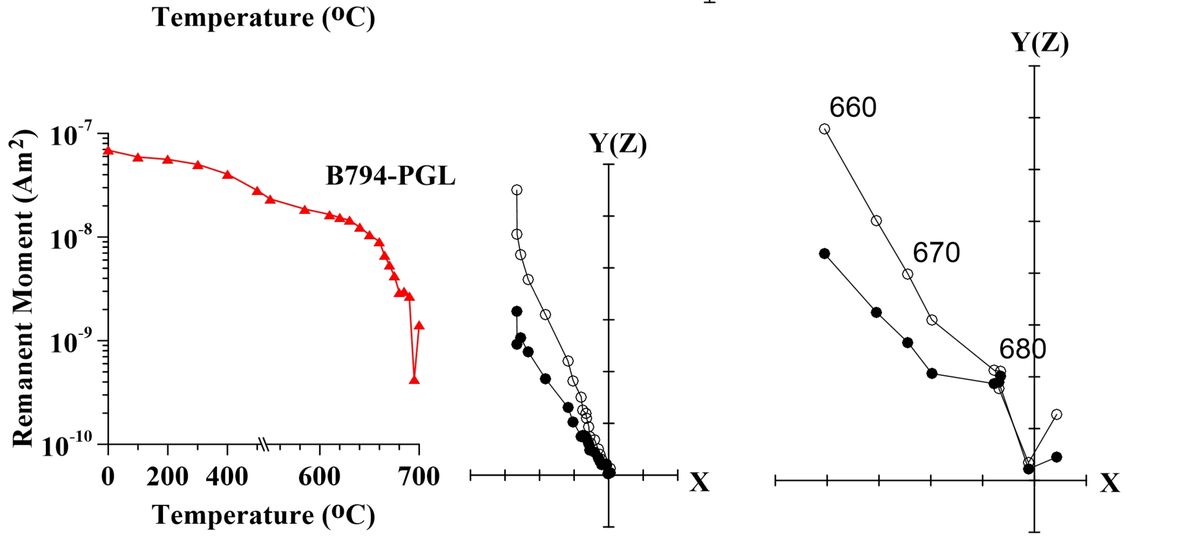

(q)

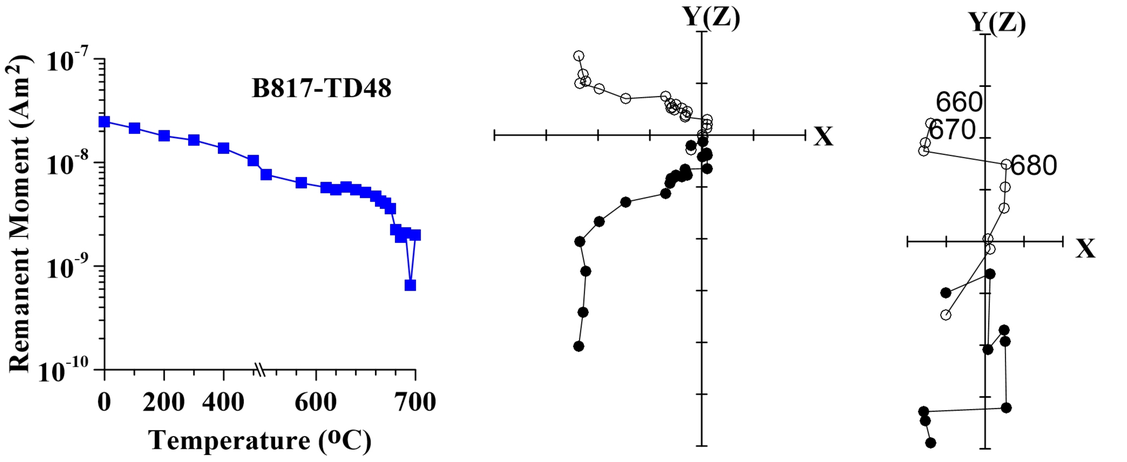

(r)

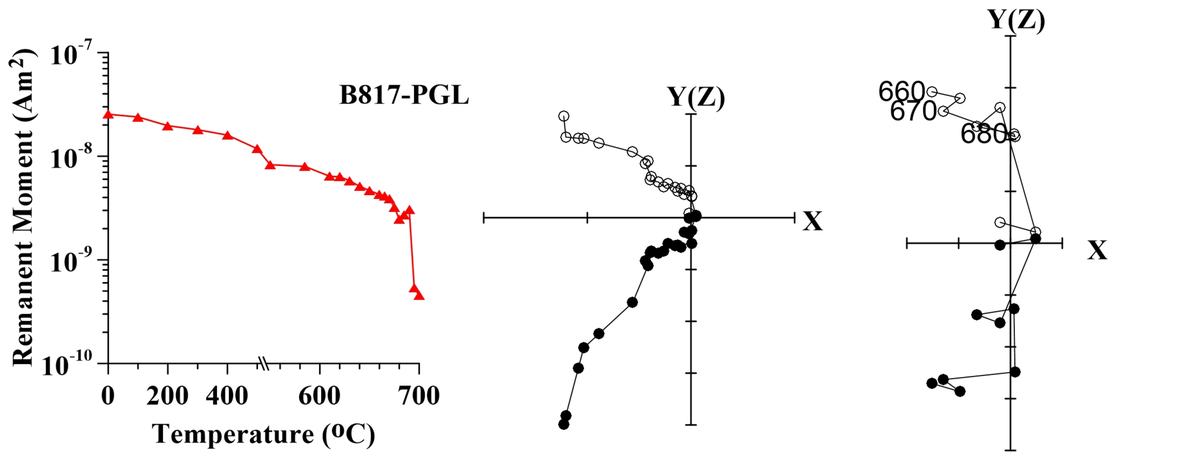

(s)

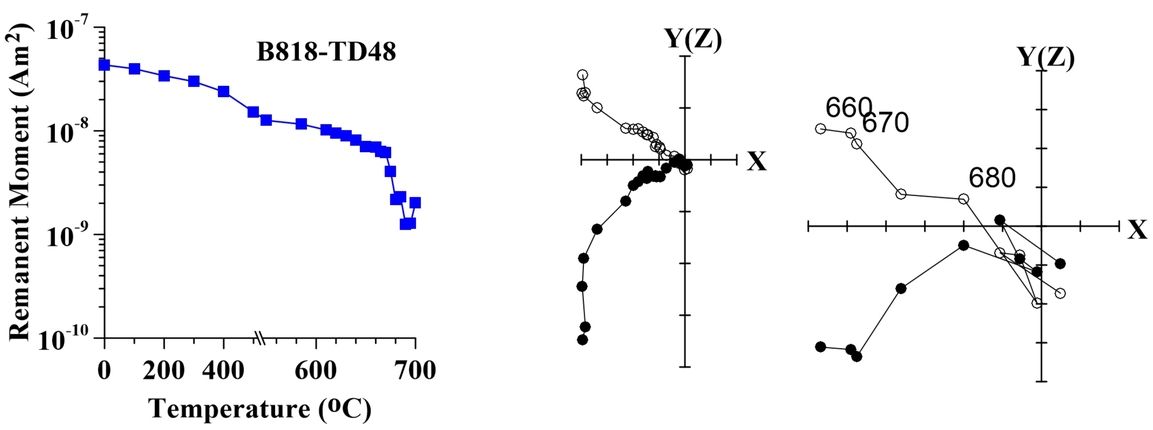

(t)

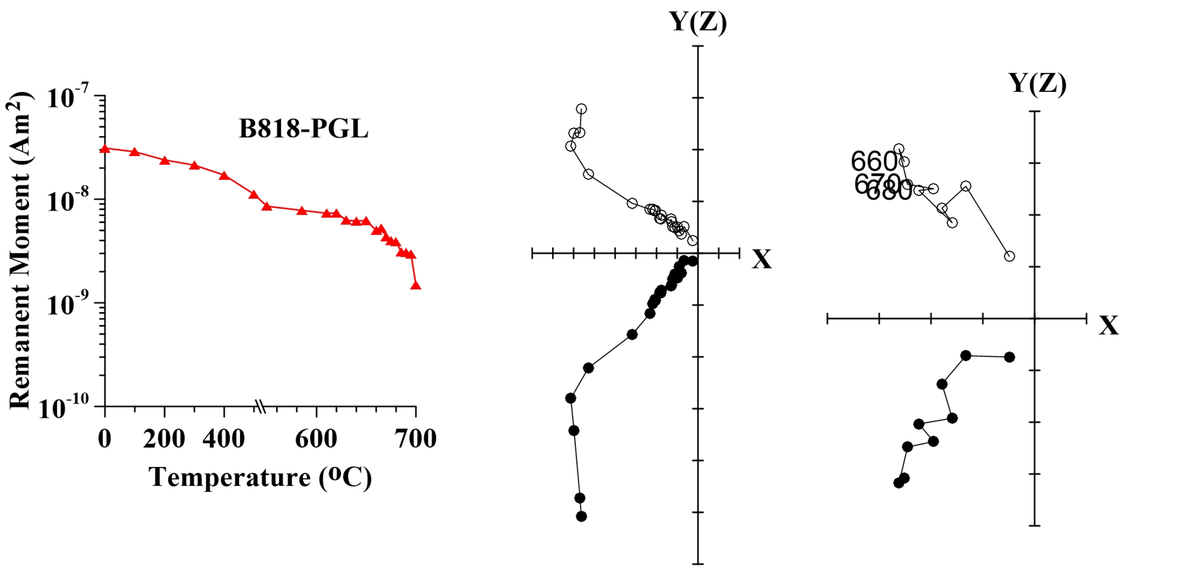

(u)

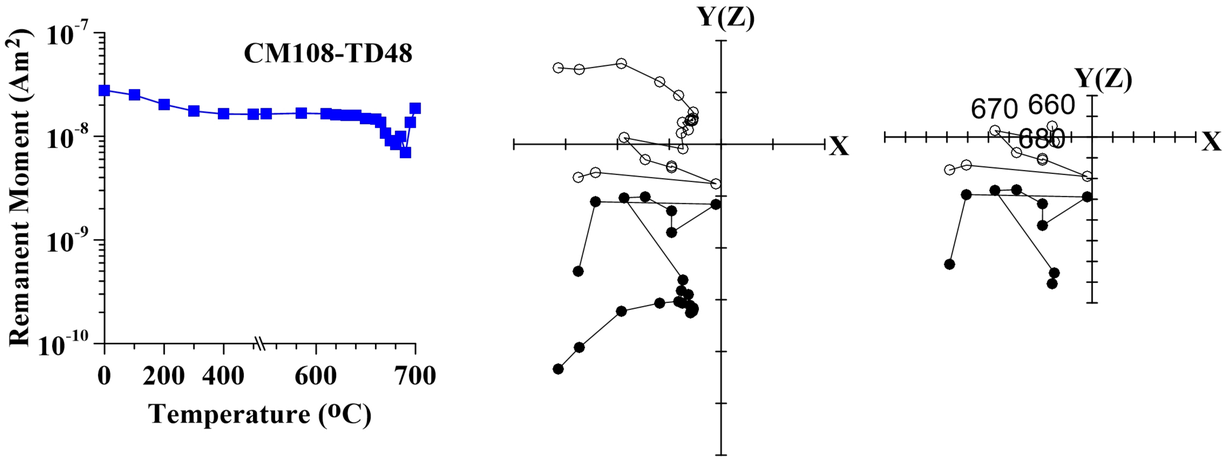

(v)

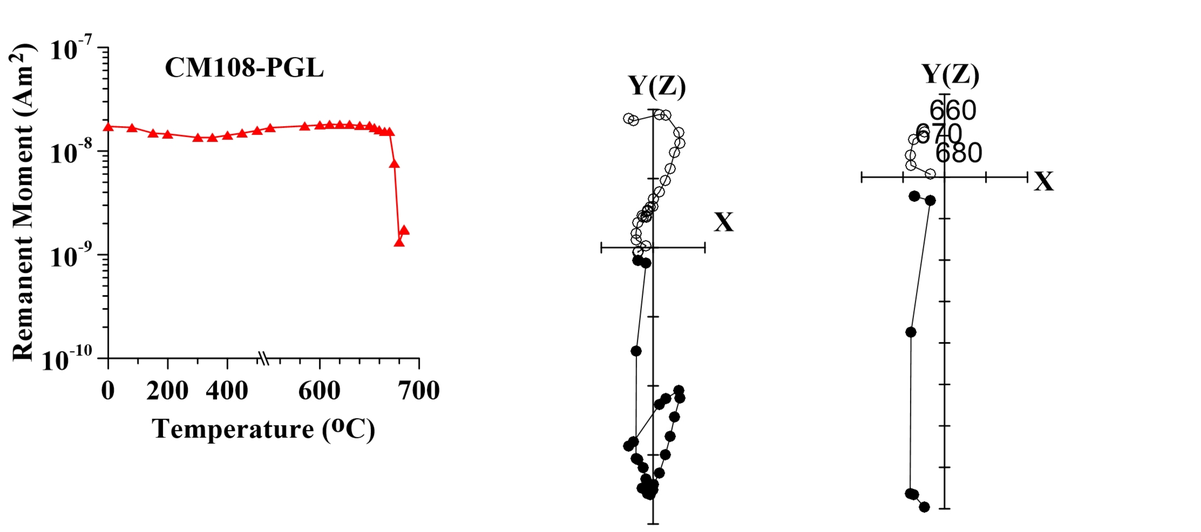

(w)

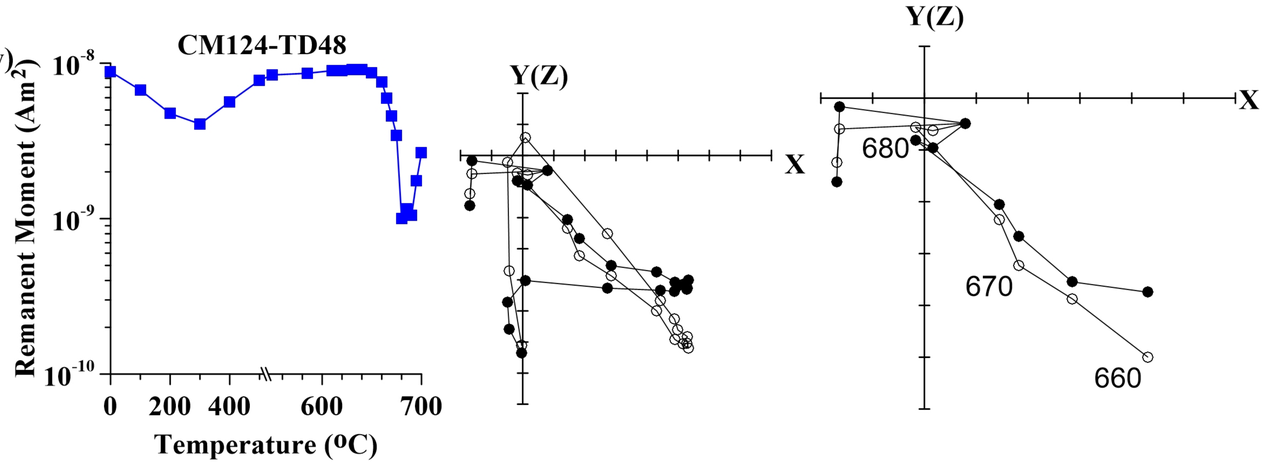

(x)

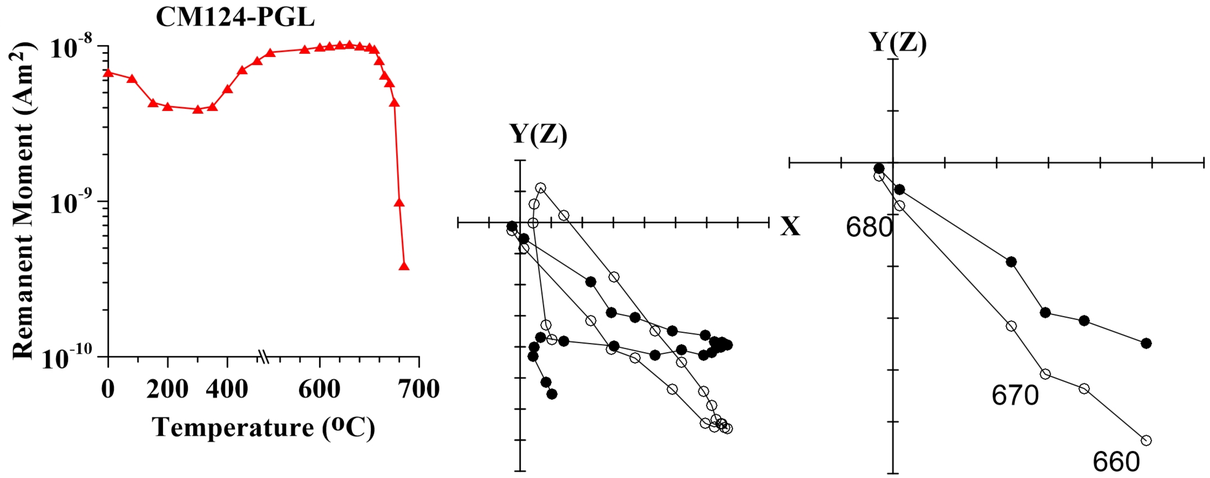

Figure S1.

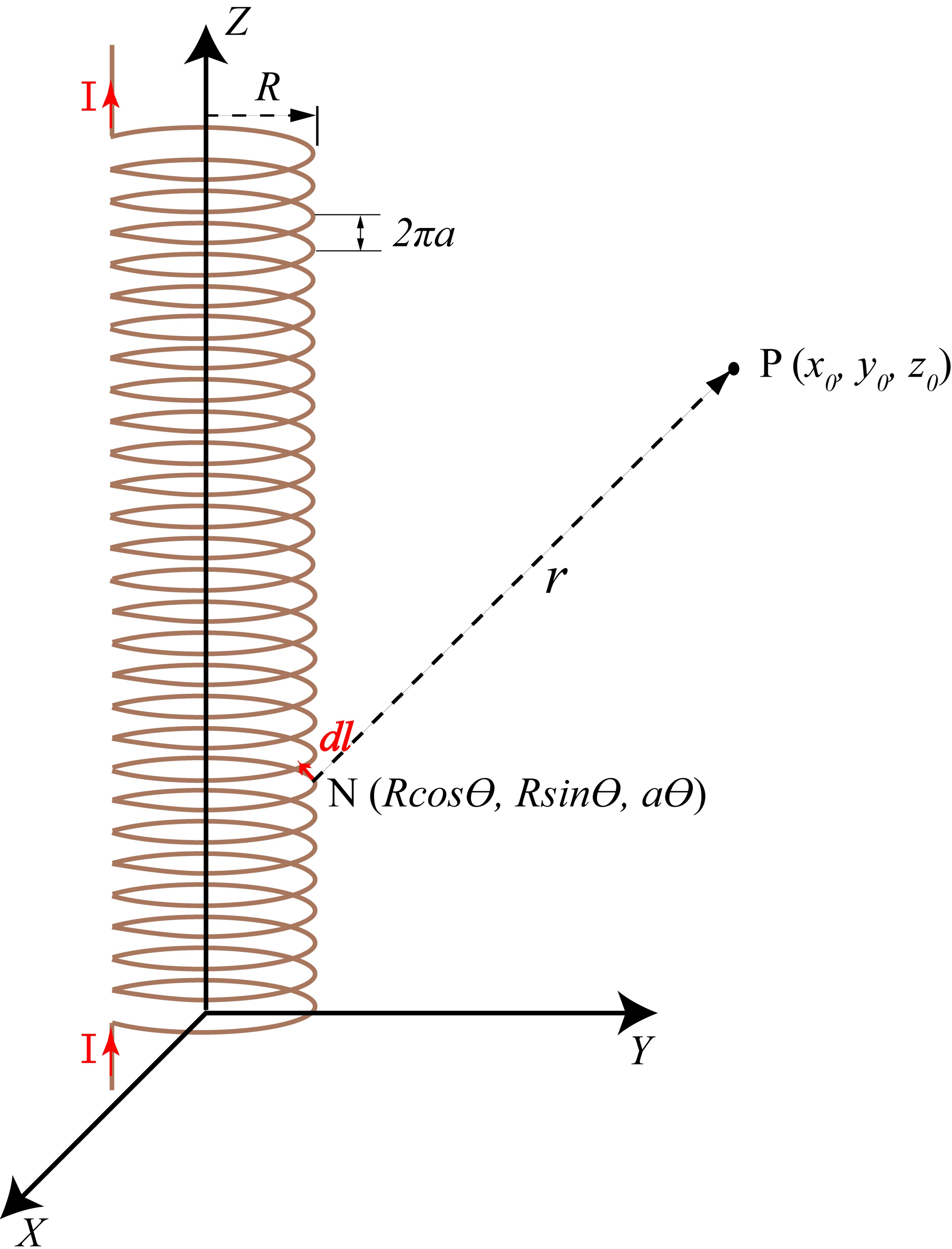
Z
R
I
2πa
P (x0, y0, z0)
r
dl
N (Rcosϴ, Rsinϴ, aϴ)
I
Y
X

Figure S2.

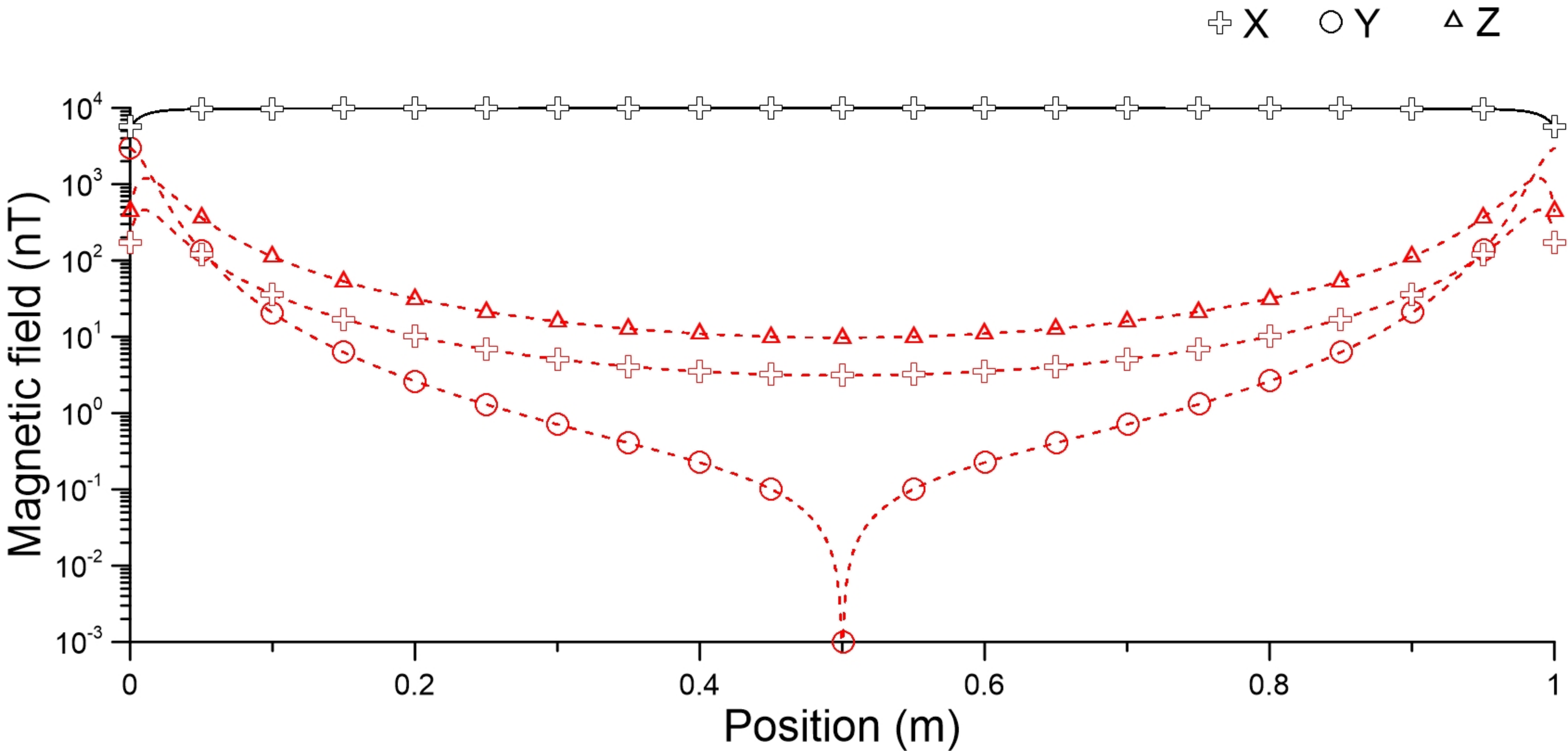
X
Y
Z
Magnetic field (nT)
10^4
10^3
10^2
10^1
10^0
10^{-1}
10^{-2}
10^{-3}
0
0.2
0.4
0.6
0.8
1
Position (m)

Figure S3.

(a)

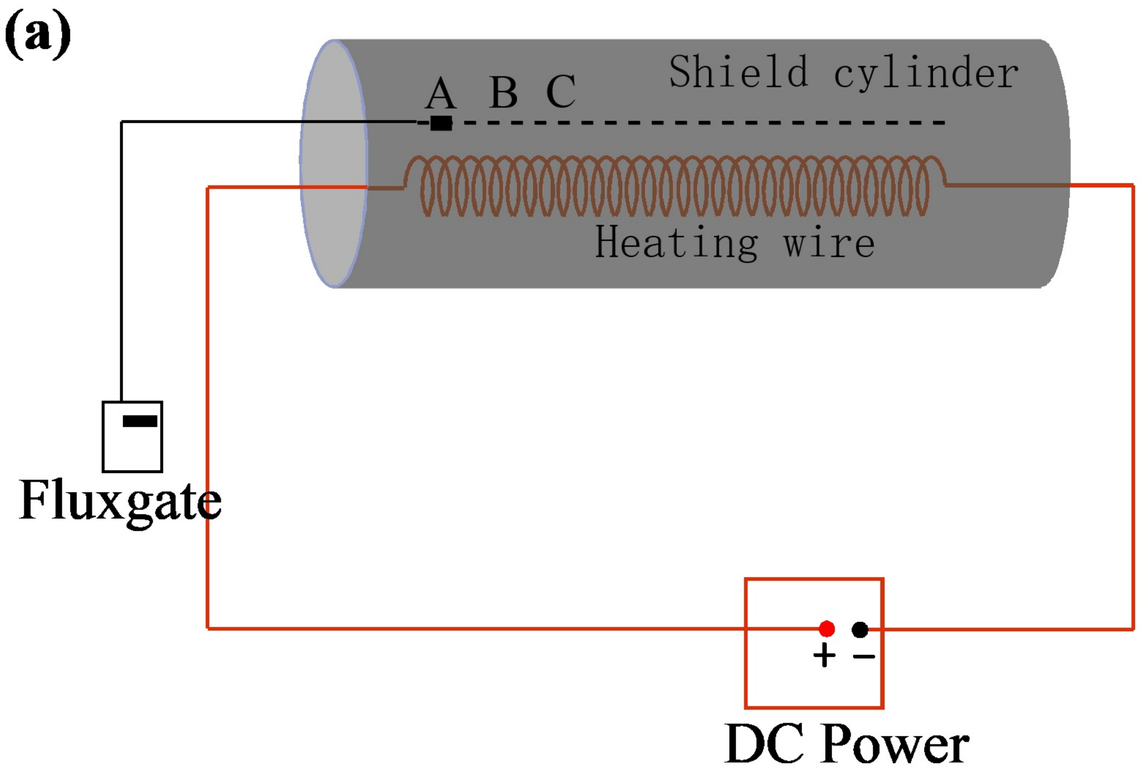
A B C
Shield cylinder
Heating wire
Fluxgate
+ −
DC Power

(b)

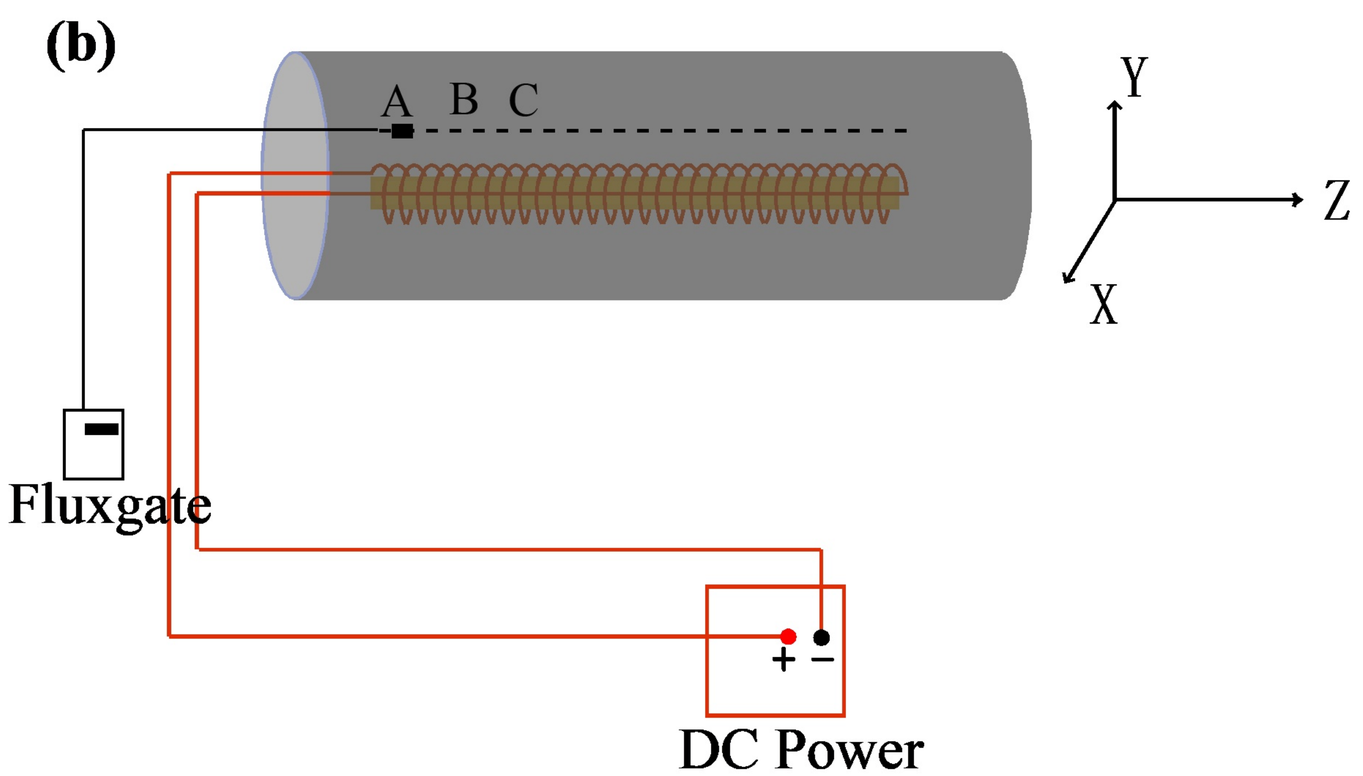
A B C
Y
Z
X
Fluxgate
+ −
DC Power

(c)

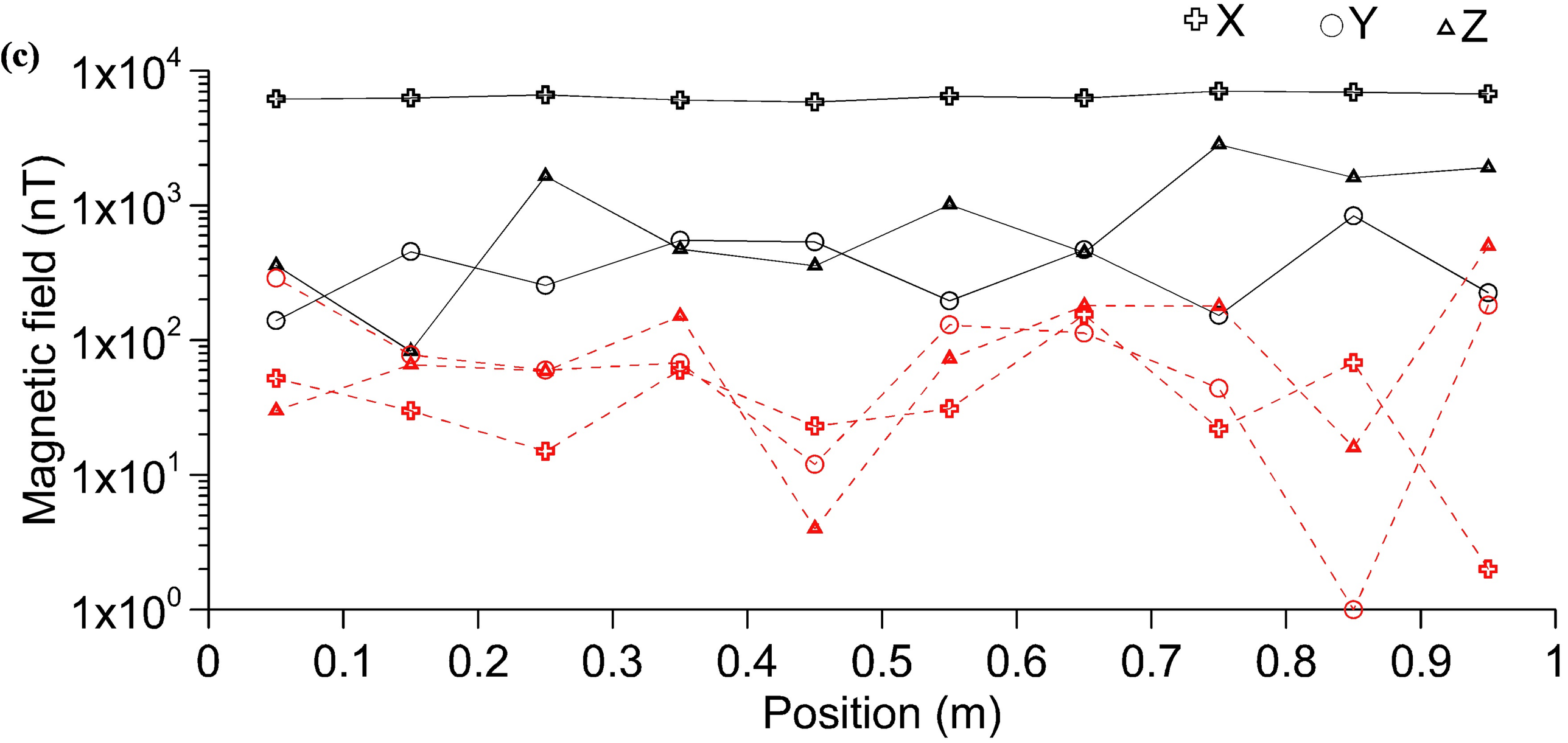
X
Y
Z
1x10^4
1x10^3
1x10^2
1x10^1
1x10^0
Magnetic field (nT)
0
0.1
0.2
0.3
0.4
0.5
0.6
0.7
0.8
0.9
1
Position (m)

Figure S4.

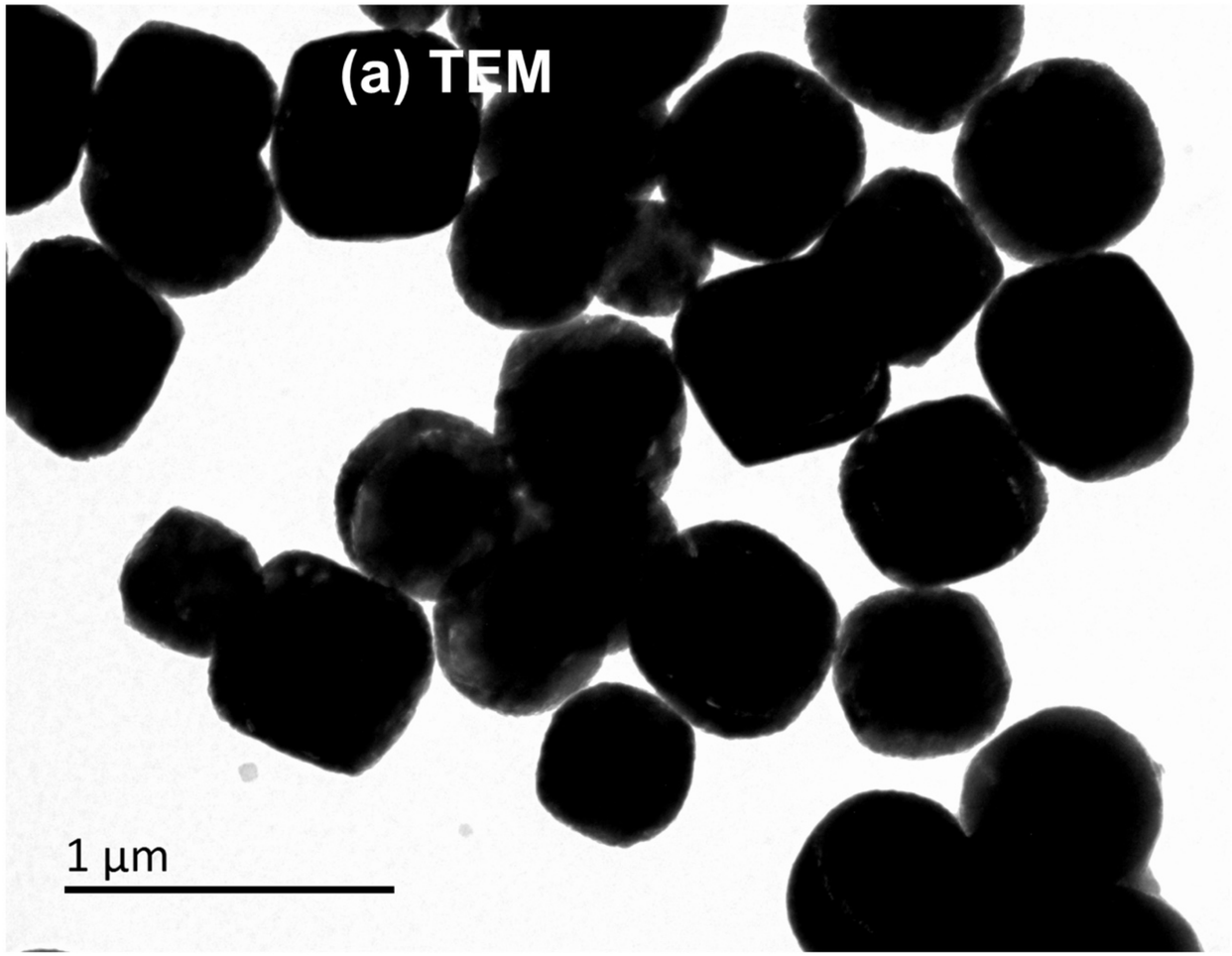
(a) TEM
1 μm

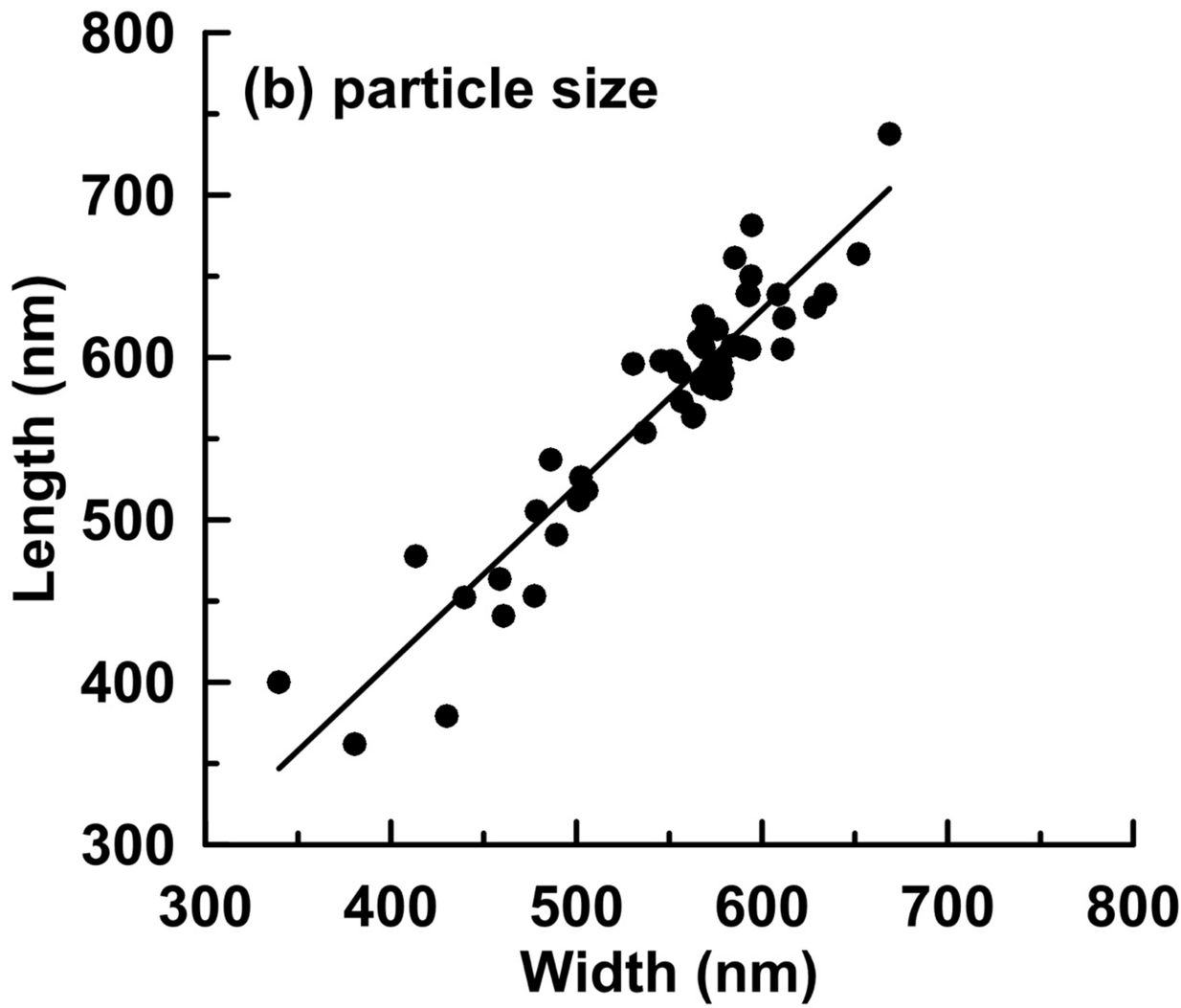
(b) particle size
Length (nm)
Width (nm)
300
400
500
600
700
800

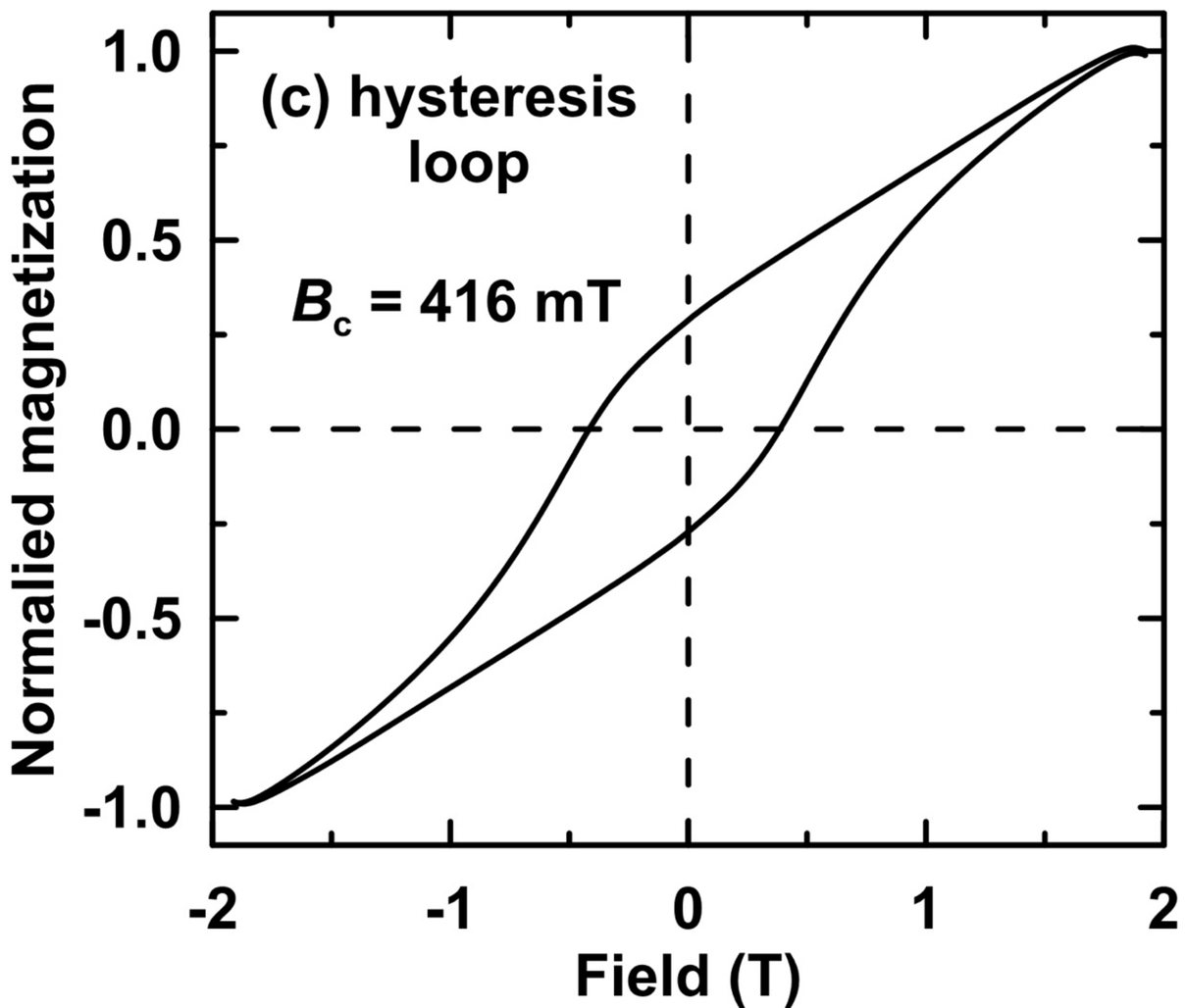
(c) hysteresis loop
B_c = 416 mT
Normalied magnetization
Field (T)
1.0
0.5
0.0
-0.5
-1.0
-2
-1
0
1
2

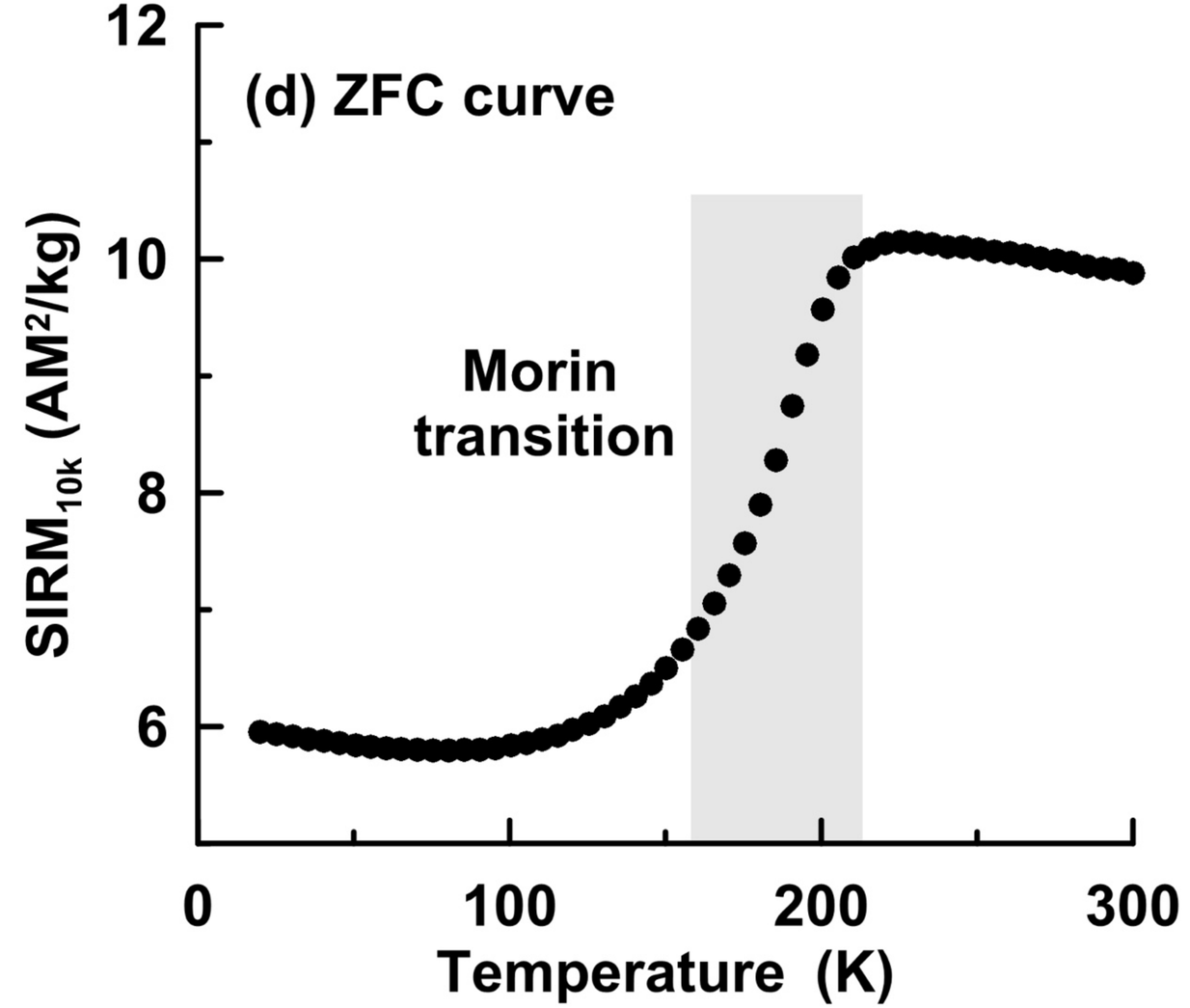
(d) ZFC curve
Morin transition
$SIRM_{10k}$ (AM^2/kg)
Temperature (K)
12
10
8
6
0
100
200
300